



IMPROVED TOUGHNESS OF REFRACTORY COMPOUNDS

by

T. R. Wright and D. E. Niesz

BATTELLE
Columbus Laboratories

Reproduced by
NATIONAL TECHNICAL
INFORMATION SERVICE
US Department of Commerce
Springfield, VA. 22151

prepared for

NATIONAL AERONAUTICS AND SPACE ADMINISTRATION

NASA Lewis Research Center
Contract NAS 3-17766
Cleveland, Ohio 44135

(NASA-CR-134690) IMPROVED TOUGHNESS OF
REFRACTORY COMPOUNDS (Battelle Columbus
Labs., Ohio.) CSCL 11D

N74-34069

Unclas
G3/18 49323

IMPROVED TOUGHNESS OF REFRACTORY COMPOUNDS

by

T. R. Wright and D. E. Niesz

BATTELLE
Columbus Laboratories

prepared for
NATIONAL AERONAUTICS AND SPACE ADMINISTRATION

NASA Lewis Research Center
Contract NAS 3-17766
Cleveland, Ohio 44135

1. Report No. CR-134690		2. Government Accession No.		3. Recipient's Catalog No.	
4. Title and Subtitle IMPROVED TOUGHNESS OF REFRACTORY COMPOUNDS (U)				5. Report Date October 11, 1974	
				6. Performing Organization Code	
7. Author(s) T. R. Wright and D. E. Niesz, Battelle Columbus Laboratories				8. Performing Organization Report No.	
9. Performing Organization Name and Address BATTELLE Columbus Laboratories 505 King Avenue Columbus, Ohio 43201				10. Work Unit No.	
				11. Contract or Grant No. NAS 3-17766	
12. Sponsoring Agency Name and Address National Aeronautics and Space Administration Washington, D.C. 20546				13. Type of Report and Period Covered Contractor Report	
				14. Sponsoring Agency Code	
15. Supplementary Notes Project Manager: Dr. Thomas P. Herbell NASA-Lewis Research Center Cleveland, Ohio 44135					
16. Abstract The concept of "grain-boundary-engineering" through elimination of the grain-boundary silicate phase in silicon nitride was developed. The process involved removal of the natural-occurring silica from the nitride powder via a thermal treatment coupled with the use of nitride additives to compensate the remaining oxygen. Magnesium and aluminum nitrides were found to be the most effective additive for use as oxygen compensators. Magnesium nitride could also be utilized as a densification aid; however, aluminum nitride containing materials required the extra addition of alumina to achieve high density by hot pressing. Although these engineered materials exhibited little or no improvement in impact strength over previously developed materials, the elevated temperature mechanical behavior of the structures were greatly enhanced. Strength decreases at elevated temperatures were not observed in the alumina containing material. The creep rate of a dual additive sialon composition was two orders of magnitude lower at 1400 C than commercial silicon nitride. A cursory analysis of the creep mechanism indicated that grain-boundary sliding was avoided through elimination of the grain-boundary silicate phase. PRICES SUBJECT TO CHANGE					
17. Key Words (Suggested by Author(s)) Silicon Nitride Sialon Grain Boundary Engineering High Purity Processing Hot Pressing Impact Strength Flexure Strength Creep				18. Distribution Statement Unclassified - Unlimited	
19. Security Classif. (of this report) Unclassified		20. Security Classif. (of this page) Unclassified		21.	

* For sale by the National Technical Information Service, Springfield, Virginia 22151

FOREWORD

The following report was prepared by personnel of Battelle's Columbus Laboratories, Columbus, Ohio, and describes original work performed under Contract NAS 3-17766.

The work was done under the management of Dr. T. P. Herbell, Materials and Structures Division, NASA-Lewis Research Center.

The studies described herein were performed in the Ceramic Materials Section of the Inorganic Materials Department, Battelle's Columbus Laboratories. Dr. T. R. Wright served as Principal Investigator. Selected impact testing was performed by Dr. T. Vasilos of AVCO Corporation, Systems Division. Reported creep values were measured by Dr. M. S. Seltzer of BCL's High Temperature Materials and Processes Section.

The contract was performed over the period July 1, 1973 to May 31, 1974.

TABLE OF CONTENTS

	<u>Page</u>
ABSTRACT	1
SUMMARY.	1
INTRODUCTION	3
EQUIPMENT AND INERT PROCESSING	6
EXPERIMENTAL STUDIES	7
I. MATERIALS SELECTION	7
II. MATERIALS PURIFICATION	10
Purification Studies.	10
Powder Characterization	17
Summary of Treatment Results	17
III. ADDITIVE EVALUATION	21
Materials Preparation	21
Pure Silicon Nitride.	22
Nitride Additives	22
Oxide Additives	23
Dual Additive Approach.	26
IV. MATERIAL EXAMINATION	28
Magnesium Nitride Additives	28
Magnesium Oxide Additives	30
Dual Additive Materials	33
V. TEST BILLET CONSOLIDATION	37
VI. INITIAL TESTING	42
Impact Tests	42
Additional Tests	42
VII. BILLET REFINEMENT	46
VIII. FINAL IMPACT TESTING	49
IX. LARGE SPECIMEN IMPACT TESTS	49
X. STRUCTURE CHARACTERIZATION	52
XI. ADDITIONAL PROPERTY STUDIES	58
DISCUSSION OF RESULTS.	62
CONCLUSIONS	69
RECOMMENDATIONS	70
REFERENCES	72

LIST OF TABLES

	<u>Page</u>
Table 1. Characterization Data for As-Received Si_3N_4 Powders	8
Table 2. Purification Rate of Various Powder Samples at 1600 C Under 4×10^{-3} MN/m ² (30 TORR N ₂)	14
Table 3. Oxygen Removal for Various Powders Following 16 Hours at 1600 C Under 4×10^{-3} MN/m ² (30 MM of Hg) NITROGEN OVER PRESSURE . . .	15
Table 4. Summary of Nitride Additive Hot-Pressing Studies	24
Table 5. Composition and Density Data for Initial Impact Specimens	41
Table 6. Initial Impact Test Results	43
Table 7. Composition and Selected Property Data for Initial Impact Specimens	44
Table 8. Refined Compositions for Second Impact Tests	47
Table 9. Final Impact Strengths	50
Table 10. Charpy Impact Values for Large Specimens of G-20AlON	51
Table 11. Impurity and Oxygen Analysis of Final Impact Bar Composition . . .	53

LIST OF FIGURES

Figure 1. Gas Phase Partial Pressure Relationships from Potential Reactions	11
Figure 2. Oxygen Removal Rate at Indicated Pressure and Temperature	13
Figure 3. Percent Oxygen Removed at 1600 C Under 4×10^{-3} MN/m ² Nitrogen (~ 30 Torr)	16
Figure 4. Effect of Thermal Purification Treatment on Silicon Nitride Powder	18
Figure 5. Effect of Heat Treatment on Particle Size Distribution	19
Figure 6. Effect of Magnesium Nitride Addition on Si_3N_4	29

V

List of Figures - (Cont.)

	<u>Page</u>
Figure 7. Fracture Surface of Si_3N_4 Containing Mg_3N_2 Additive. . . .	31
Figure 8. Composition MO-1 Microstructures	32
Figure 9. Dual Additive Sialon, Composition 20AlON	34
Figure 10. Composition 20-AlON Prepared from Material F	35
Figure 11. Time-Density Relationship for Hot-Pressing Si_3N_4 - Mg_3N_2 Test Billets	38
Figure 12. Time-Density Relationship for Hot-Pressing Si_3N_4 -AlN- Al_2O_3 Test Billets	39
Figure 13. Composition G-MN-1	54
Figure 14. Composition G-20AlON	56
Figure 15. Composition G-35AlON	57
Figure 16. Flexure Strength as a Function of Temperature	59
Figure 17. Creep Behavior in Air of BCL G-20AlON Sialon Compared with That of Commercial Silicon Nitride.	61
Figure 18. Strength Behavior of Si_3N_4 with Mg_3N_2 Additive as a Function of Initial Powder Oxygen Content	64
Figure 19. High-Oxygen Silicon Nitride Containing Magnesium Nitride Additive	65

IMPROVED TOUGHNESS OF REFRACTORY COMPOUNDS

by

T. R. Wright and D. E. Niesz

ABSTRACT

The concept of "grain-boundary-engineering" through elimination of the grain-boundary silicate phase in silicon nitride was developed. The process involved removal of the natural-occurring silica from the nitride powder via a thermal treatment coupled with the use of nitride additives to compensate the remaining oxygen. Magnesium and aluminum nitrides were found to be the most effective additive for use as oxygen compensators. Magnesium nitride could also be utilized as a densification aid; however, aluminum nitride containing materials required the extra addition of alumina to achieve high density by hot pressing.

Although these engineered materials exhibited little or no improvement in impact strength over previously developed materials, the elevated temperature mechanical behavior of the structures were greatly enhanced. Strength decreases at elevated temperatures were not observed in the alumina containing material. The creep rate of a dual additive sialon composition was two orders of magnitude lower at 1400 C than commercial silicon nitride. A cursory analysis of the creep mechanism indicated that grain-boundary sliding was avoided through elimination of the grain-boundary silicate phase.

SUMMARY

In this study, an approach of refinement and iteration within the framework of a developed process was utilized with the objective of improving the impact strength of silicon nitride. The objective of the study was to improve the material through elimination of strength limiting flaws common to most commercially available grades of material. The strength limiting flaw of major concern was the silicate grain-boundary phase formed from the reaction of the

silica passivation layer on the surface of the silicon nitride powder and the additives commonly used to promote densification.

By a developed thermal treatment, it was possible to remove approximately 50 percent of the natural-occurring oxide from the as-received powder. Using this heat treated powder, both Mg_3N_2 and AlN were found to perform as oxygen compensation additives for removal of the remaining oxygen from the system. It was found necessary to use the additive in stoichiometric amounts based on the residual oxygen level.

Magnesium nitride was also found to perform as densification aid for the consolidation of silicon nitride by hot pressing. Aluminum nitride alone would not aid in densification but required the addition of Al_2O_3 to achieve high density. Such compositions were referred to as dual-additive sialons.

Structures prepared by hot pressing from the magnesium nitride compensated and dual additive sialon materials did not meet the target impact criteria of 0.68 j. The maximum impact level obtained with any material at room temperature was 0.24 j. Impact values increased slightly as a function of increasing temperature.

The dual additive sialon materials exhibited promise in the area of enhanced elevated temperature mechanical behavior. A strength decrease at elevated temperatures, common to commercial silicon nitride, was not observed. Flexure strengths in excess of 565 MN/m^2 (82,000) were observed at $\sim 1325 \text{ C}$. The creep rate of a 20 mole percent Al_2O_3 dual additive sialon was two orders of magnitude lower than a commercial grade of silicon nitride at 1400 C under a stress for 69 MN/m^2 (10,000 psi).

The concept of grain-boundary-engineering through elimination of the silicate grain-boundary phase using the techniques developed in this study was judged to be successful. The creep mechanism of grain-boundary sliding caused by the viscous grain-boundary silicate phase was avoided in the engineered dual additive sialons. It is believed that further improvements are possible, particularly in the area of impact performance, through continued development of these materials.

INTRODUCTION

Increased service demands in turbine engines have identified major materials needs in terms of fabricability, strength, and oxidation resistance for turbine blades and stator vanes. Current metallic materials, i.e., super-alloys, are satisfactory at temperature levels currently experienced; however, as service demands are increased in advanced engines, the need for higher temperature materials has become evident.

At temperatures of 1350 C and greater, the use of metallic and coated metallic components will be limited due to the lack of elevated-temperature oxidation resistance. The development of silicon-containing refractory structural components provides a means of avoiding the oxidation problem in that a protective film of silica is formed on the surface. As a result, Si_3N_4 is receiving increased attention for use in these applications. This material has been shown to be thermally stable at the temperatures in question and, due to the high strength and relatively low thermal expansion behavior, exhibits good thermal shock resistance.

As with most ceramic materials when considered for turbine applications, low impact resistance is a problem area. Improved design criteria will avoid many problems; however, the use of ceramic components in turbine applications will never achieve their full potential without improvements in the behavior characteristics of the materials themselves. As a result, the objective of this program was to develop an improved Si_3N_4 -base ceramic for hot flow path components in advanced aircraft turbine engines with emphasis on developing a tougher, more impact resistant material.

The initial specific goal of the program was to obtain an impact resistance of 0.68 joules (6 in-lb) at all temperatures to 1325 C as measured by a Charpy test on unnotched bars 6.4 by 6.4 mm (0.25 by 0.25 in) in cross section over a 38.8 mm (1.5 in) span. Increased impact resistance was not to be achieved at the expense of other properties important to the service performance of the material, such as stress-rupture strength, thermal-shock resistance, and thermal stability.

The theory behind increasing the impact strength of silicon nitride in this program was developed from fundamental considerations of the phenomenon of fracture in ceramic materials. Concepts for the approach followed were derived from the criteria that, in an impact test, sufficient elastic energy must be impacted to stress the specimen locally to its fracture stress. Therefore, the basic approach followed to improve the impact strength was to maximize the fracture stress at all temperatures through elimination of the strength limiting flaws in the microstructure.

According to the present state of the art, high-density silicon nitride is prepared by hot pressing using a densification aid. Magnesium oxide, MgO , has been the primary densification aid utilized to date in commercially available materials, although several studies are currently being conducted to evaluate or identify other additive systems which show potential for improving silicon nitride properties or fabricability.

The primary shortcoming of currently available high-density silicon nitride is its low strength and stress rupture resistance at elevated temperatures. This limitation is not believed to be inherent to Si_3N_4 ; rather, it results from an oxide or silicate phase present at the grain boundaries. According to Wild, et al.,^{(1)*} the magnesia added as a densification aid will react with SiO_2 present on the surface of the nitride particles to form a magnesium silicate. Since this grain boundary phase melts or softens at a relatively low temperature, failure occurs by a grain boundary sliding mechanism.⁽²⁾ Other impurity cations present in the system will affect the strength, mainly through lowering the viscosity of the silicate phase, i.e., calcium.⁽³⁾

The effect of the silicate grain boundary phase on the room temperature mechanical properties may be open to question. It is postulated that the existence of a continuous brittle second phase will reduce the resistance to crack propagation by providing a continuous path for extremely rapid critical crack growth as well as sites for crack initiation. While measurements confirming this hypothesis have not been made, it is believed that elimination of the grain boundary phase should improve the room temperature mechanical performance of silicon nitride as well as the elevated temperature properties.

* References are listed on page 72.

The basic approach utilized on this program was one of grain boundary engineering or modifying the grain boundaries of silicon nitride in such a manner as to eliminate the major strength limiting flaw; i.e., the grain boundary silicate phase.

In order to eliminate silicate from the grain boundary, two basic concepts were proposed.

- (1) Start with a relatively pure, low-oxygen, material and remove the oxide passivation layer from the powder through a series of thermal treatments. Following the heat treatment, the powder must be handled in a controlled atmosphere to prevent subsequent recontamination.
- (2) Select additives that will serve as densification aids and, at the same time, allow the remaining oxygen to be taken into solid solution in the silicon nitride lattice.

The above concept of grain boundary engineering was utilized in the following program in an attempt to increase the toughness of the material through elimination of the strength-limiting flaws. The program was conducted in a sequence of eight experimental tasks as follows:

- (1) Materials Selection
- (2) Materials Purification
- (3) Additive Evaluation
- (4) Material Examination
- (5) Test Billet Consolidation
- (6) Impact Testing
- (7) Refinement
- (8) Impact Testing.

In addition, preliminary measurement of selected elevated temperature properties were performed. The above are described in detail in the following report.

EQUIPMENT AND INERT PROCESSING

In order to maintain the oxygen-free, high-purity conditions required on this program, all processing was performed in inert-atmosphere glove box systems. The systems employ an argon atmosphere which is maintained at a dew point of minus 90 C (~ 1 ppm H_2O) and an oxygen level of ~ 5 ppm.

In addition to comminution facilities for ball milling, the glove box system is connected to a tungsten mesh furnace for heat treatment of the powders. This programed system can be evacuated to a level of 10^{-9} to 10^{-10} MN/m² at temperature of 2300 C. The nitrogen supply utilized in all heat treatments was a prepurified grade of 99.99 percent purity. It was not necessary to expose the powders to the ambient atmosphere from the point they were received until consolidated into dense structures.

For hot pressing, the material was loaded into preoutgassed, tantalum-lined, graphite dies in the glove box chamber and the assembly sealed. The die arrangement was transferred to the hot pressing assembly where it was evacuated to 10^{-9} MN/m² prior to backfilling with prepurified nitrogen (5×10^{-2} MN/m²). The transfer techniques were essentially those developed for hot pressing high-purity hydride materials; therefore, it is believed that no contamination occurred in this operation.

Heating was performed by induction coupling with the die material. Additive evaluations and densification parametric studies were performed in units having a 0.133 MN (15 ton) load capacity. Billet fabrication was conducted in a 0.665 MN (75 ton) load limit unit. The specimen deformation could be monitored throughout the densification cycle by means of dilatometers attached to the hydraulically activated rams.

EXPERIMENTAL STUDIES

I. MATERIALS SELECTION

As mentioned earlier, it is believed that high oxygen levels and certain types of impurities in the commercial starting powders may be responsible for the strength limiting grain boundary phases present in consolidated structures. In order to obtain as pure a starting powder as possible for use on the program, commercial sources of powder were screened and characterized. Powder characterizations included surface area, particle size distribution, oxygen content, phase purity, impurity content, and powder morphology. Based on the results of these characterizations, a commercial grade of powder was selected for use on the program.

A total of fifteen (15) commercial vendors of silicon nitride powder were contacted as potential sources of material. On the basis of availability, particle size, stated purity, and cost, seven different grades of commercial material were selected, procured, and characterized.*

Upon receipt of the material, each was transferred to a high-purity inert-gas glove box to maintain the as-received purity and chemistry of the powders. Each powder was sampled and submitted for the appropriate characterization analysis. The characterizations and the techniques utilized are as follows:

Impurity Content	- Emission Spectroscopy
Oxygen Content	- Inert Gas Fusion
Phase Purity	- X-ray Diffraction
Surface Area	- Modified BET
Size Distribution	- Centrifugal Sedimentation (MSA).

Characterization results obtained on commercial powders are shown in Table 1. Based on the results of these characterizations, and the availability of the powder, materials B, F, and G, were utilized at various times on the program.

* Material A: Atlantic Equipment Engineers
Material B: Cerac, Inc. - Electronic Grade
Material C: Advanced Materials Engineering - Super Grade
Material D: Advanced Materials Engineering - Grade CP-75
Material E: Varlacoid Chemical Co.
Material F: Shieldalloy Corp. - White Grade
Material G: Montecatini Edison.

TABLE 1. CHARACTERIZATION DATA FOR AS-RECEIVED Si_3N_4 POWDERS

	Major Impurity Content, ppm										Oxygen Content, weight percent	X-Ray Analysis, percent		Surface Area, m^2/g	Particle Size, μm
	Al	Ca	Co	Cr	Fe	Mg	Mo	Ni	Ti	W		α	β		
A	1000	1000	200	400	6000	30	200	300	200	1000	2.52 2.62 2.70 <u>2.62*</u>	20	80	2.36	Max = 40 Min = 0.6 Med = 7.0
	Total Purity = 99.89 percent														
B	2000	500	10	20	20	30	10	10	10	50	1.64 1.65 1.58 <u>1.62*</u>	15	85	1.92	Max = 60 Min = 0.2 Med = 8.6
	Total Purity = 99.71 percent														
C	2000	2000	10	200	4000	100	30	200	200	50	1.44 1.46 1.56 <u>1.49*</u>	20	80	3.05	Max = 25 Min = 0.2 Med = 7.5
	Total Purity = 99.08 percent														
D	3000	2000	20	50	4000	100	100	200	200	50	1.47 1.87 1.88 <u>1.91*</u>	65	35	3.80	Max = 60 Min = 0.2 Med = 6.8
	Total Purity = 98.9 percent														

TABLE 1. (Continued)

	Major Impurity Content, ppm										Oxygen Content, weight percent	X-Ray Analysis, percent		Surface Area, m ² /g	Particle Size, μ m
	Al	Ca	Co	Cr	Fe	Mg	Mo	Ni	Ti	W		α	β		
E	1000	1000	100	400	3000	50	200	200	200	1000	2.31 2.43 2.48 <u>2.41*</u>	25	75	2.50	Max = 50 Min = 0.2 Med = 7.9
Total Purity = 99.20 percent															
F	3000	800	N.D.	N.D.	80	100	N.D.	10	20	N.D.	2.77 2.78 2.78 <u>2.78*</u>	20	80	3.11	Max = 30 Min = 0.2 Med = 7.0
Total Purity = 99.58 percent															
G	1000	200	<10	<20	50	30	<10	<10	10	<50	0.47 0.46 0.46 <u>0.46*</u>	25	75	3.95	Max = 30 Min = 0.2 Med = 7.9
Total Purity = 99.40 percent															

N.D. = Not detected

* = Average value

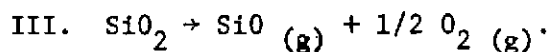
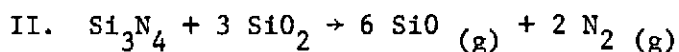
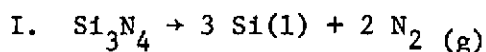
II. MATERIALS PURIFICATION

Purification Studies

The high-purity processing approach utilized in this study was dependent upon starting with an oxide-free powder then handling the material in such a manner as to prevent contamination during subsequent processing and consolidation. As shown in Table 1, completely oxygen-free powders are not available from commercial sources. As a result, it became necessary to remove the oxygen from the powders as completely as possible by a high temperature heat treatment.

Presently available powders contain oxygen as a passivation layer in the surface of the particles or as a substitution for nitrogen in the Si_3N_4 lattice. As mentioned previously, it is believed that the passivation layer of oxide leads to the formation of a silicate grain boundary phase; therefore, removal of this layer by thermal treatment should prevent formation of the grain boundary silicate phase.

In order to estimate the thermal treatment parameters which could remove the passivation layer, the thermodynamics of the possible reactions occurring under a vacuum heat treatment were determined. The reactions considered were as follows:



The partial pressures of N_2 , SiO , and O_2 gas from each of the above potential reactions are shown in Figure 1. Based on an ultimate system pressure of 10^{-9} - 10^{-10} MN/m², and a temperature of 1500-1700 C, the data indicated that it

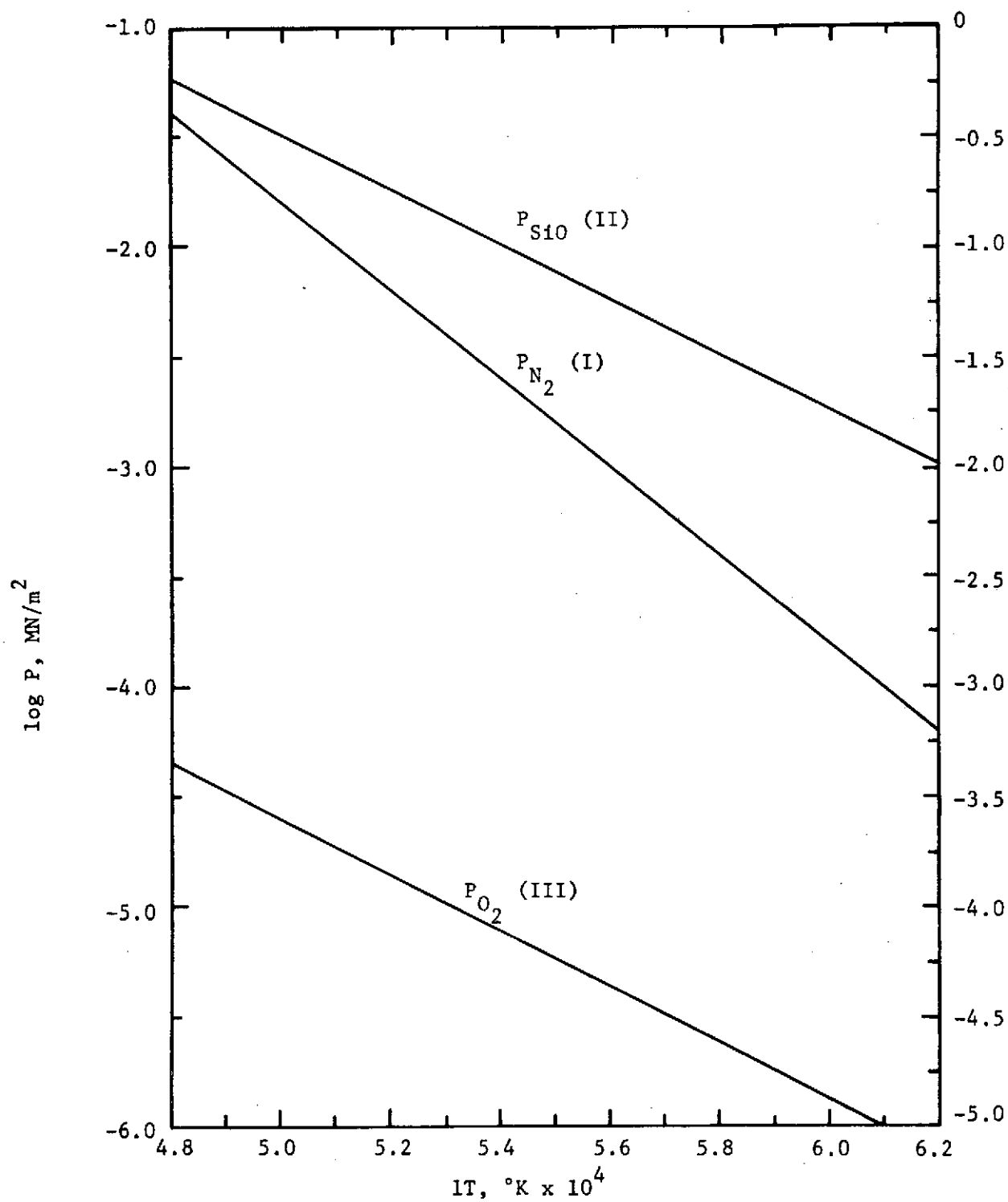


FIGURE 1. GAS PHASE PARTIAL PRESSURE RELATIONSHIPS FROM POTENTIAL REACTIONS

would be possible to remove the oxygen from the system as silicon monoxide (SiO).

To prevent decomposition of the Si_3N_4 during the vacuum distillation process, a partial pressure of nitrogen was provided. The necessary minimum pressure required was calculated on the basis of Reaction I. The pressures chosen were the exact dissociation pressures at 1500, 1600, and 1700 C (P_{N_2}) and twice the dissociation pressure at each of these temperatures ($2 P_{\text{N}_2}$) to determine the effect of nitrogen oven pressure on the oxygen removal rate.

Powder samples were heat treated in W crucibles under prepurified nitrogen (99.99 percent purity) in a W-mesh furnace attached to a glove box facility. Samples were run for 2 and 4 hour periods under the selected temperature and pressure conditions, after which the powders were analyzed for oxygen by inert gas fusion. The results of the initial purification heat treatments as performed on Material B (Cerac Electronic Grade) are shown in Figure 2 as the average oxygen removal rate at each temperature and pressure condition.

The results clearly indicate that the maximum removal rate is achieved at 1600 C under a nitrogen pressure of $4 \times 10^{-3} \text{ MN/m}^2$ (30 Torr) ($P_{\text{T}} = P_{\text{N}_2}$). Increasing the nitrogen over-pressure ($P_{\text{T}} = P_{\text{N}_2}$), appears to retard the rate of oxygen removal from the powder.

From the data, it was concluded that the kinetics of oxygen removal at 1500 C were too slow to be effective. Oxygen removal at 1700 C was believed to be retarded by powder agglomeration, possibly by sintering of the SiO_2 coating on each particle, or by solutioning of the oxide surface layer.

Heat treatments at 1600 and 1700 C resulted in a clean white powder; however, heat treatments at 1500 C with nitrogen pressures of ~ 6 and $12 \times 10^{-4} \text{ MN/m}^2$ (5 and 10 torr) resulted in some decomposition. The resultant powder was dark gray in appearance due to the presence of free silicon. Because the equilibrium nitrogen pressure is quite low at this temperature, it was believed that lack of exact control may have been responsible. For this reason, 1500 C treatments were also performed at $6.7 \times 10^{-3} \text{ MN/m}^2$ (50 torr) ($P_{\text{T}} = 10P_{\text{N}_2}$). This resulted in a clean white powder; however, the oxygen removal rate was not improved.

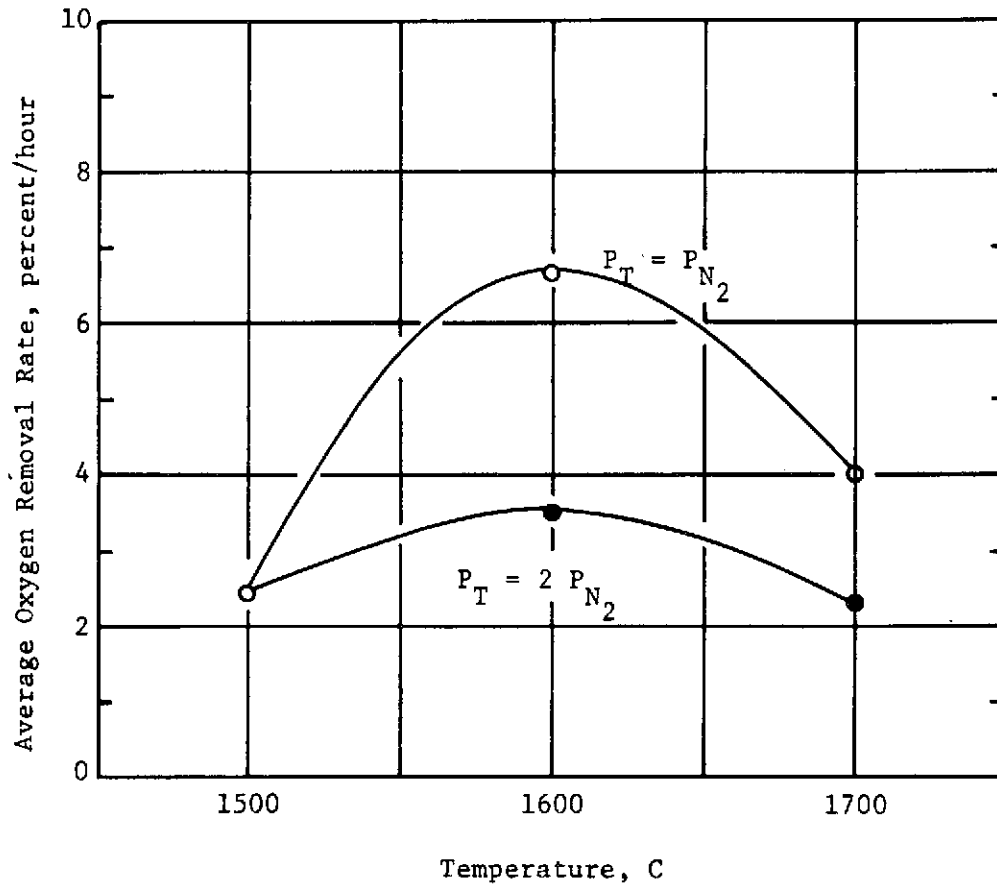


FIGURE 2. OXYGEN REMOVAL RATE AT INDICATED PRESSURE AND TEMPERATURE

(Material B-Cerac Electronic Grade)

As a result of cost considerations, it was advantageous to utilize either Materials F (Shieldalloy) or Material G (Montecatini) in the fabrication studies. In order to evaluate the use of oxygen removal of these materials, additional purification runs were performed on these materials at 1600 C and 4×10^{-3} MN/m² (30 Torr) nitrogen pressure for 2 and 4 hours. It was found that these materials behaved essentially identical to Material B (Cerac) powder as shown below.

TABLE 2. PURIFICATION RATE OF VARIOUS POWDER SAMPLES
AT 1600 C UNDER 4×10^{-3} MN/m² (30 TORR N₂)

Material	Time, hour	Reduction in Oxygen Content, percent	Oxygen Removal Rate, percent/hour
B	2	13.6	6.80
	4	25.9	6.48
F	2	14.0	7.00
	4	25.7	6.42
G	2	6.70	3.35
	4	25.20	6.30

Material G exhibits a much lower rate in the early portion of the purification treatment probably as a result of the extremely low initial oxygen level, 0.46 percent. After the initial period, the rate essentially increases to levels comparable with that of the other powders.

In order to determine the effect of heat treating time on the oxygen removal, samples of the Type F powder (Shieldalloy) were heat treated for various times at 1600 C and 4×10^{-3} MN/m² (30 Torr) nitrogen pressure. This was performed in both a static and dynamic mode for times of from 1/2 to 16 hours.

The static mode involved first evacuating the furnace system to 10^{-7} MN/m² ($\sim 10^{-6}$ Torr) and then backfilling with 4×10^{-3} MN/m² (30 Torr) total nitrogen pressure. This level of total nitrogen pressure was maintained throughout the entire heating, holding, and cooling cycle.

The dynamic purification mode involved evacuating the system to $\sim 10^{-6}$ Torr and then performing the desired thermal cycle under 4×10^{-3} MN/m² (30 Torr) of flowing nitrogen. It was thought that the SiO vapor pressure may be building up during the static cycle and preventing further vaporization of the oxide present.

The results, shown in Figure 3, indicate that a limiting oxygen level is achieved in the powder. The dynamic heat treatment progresses at a rapid rate initially (~ 13.6 percent/hour); however, removal ceases at ~ 37 percent removal. The static treatment progresses at a slower rate (~ 6.67 percent/hour); but, removal is still progressing at 8 hours. It was observed that oxide removal has essentially stopped following 16 hours of treatment at which point approximately 57.5 percent of the oxygen had been removed from the material.

The results at this point definitely indicated that it was possible to remove a considerable amount of the oxygen from the powder with a 16-hour heat treatment at 1600 C under 30 torr of nitrogen using the static heat treatment mode. In order to verify the results for other powder types, Materials B and G were also heat treated under the above condition and the oxygen content measured. The results of this experiment, as shown in Table 3, indicated that the total amount of oxygen removed varied as a function of the powder type.

TABLE 3. OXYGEN REMOVAL FOR VARIOUS POWDERS FOLLOWING 16 HOURS AT 1600 C UNDER 4×10^{-2} MN/m² (30 MM of Hg) NITROGEN OVER PRESSURE

Powder Code	Supplier	Oxygen Level, percent		Oxygen Removed, percent
		Initial	Final	
B	Cerac	1.62	0.99	45.1
F	Shieldalloy	2.78	1.18	57.5
G	Montecatini-Edison	0.46	0.24	47.8

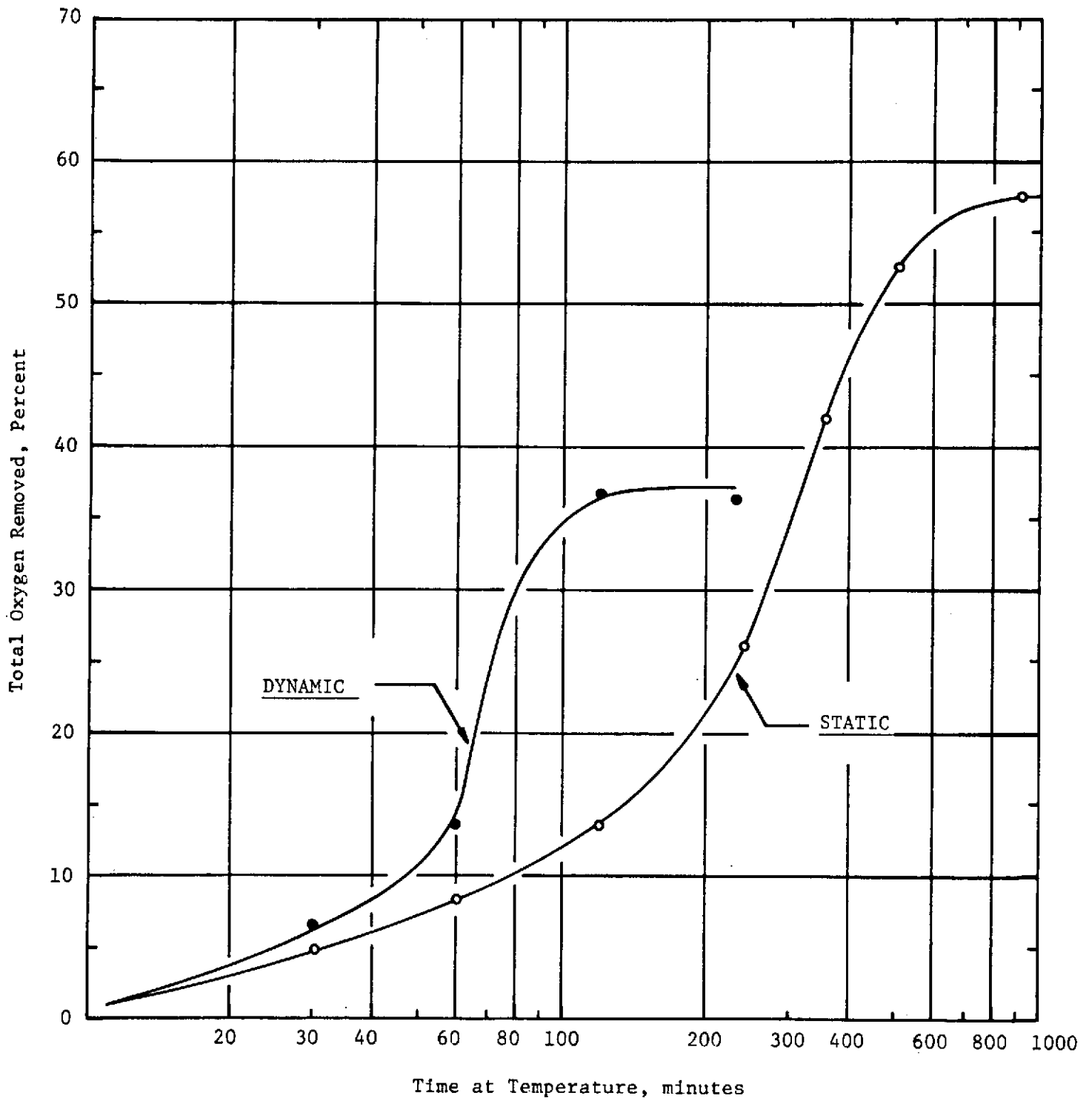


FIGURE 3. PERCENT OXYGEN REMOVED AT 1600 C UNDER 4×10^{-3} MN/m² NITROGEN (~30 TORR)
Material F-1, Shieldalloy

The experiment also pointed out the necessity of analyzing each and every powder lot prior to attempting compensation for the remaining oxygen.

Powder Characterization

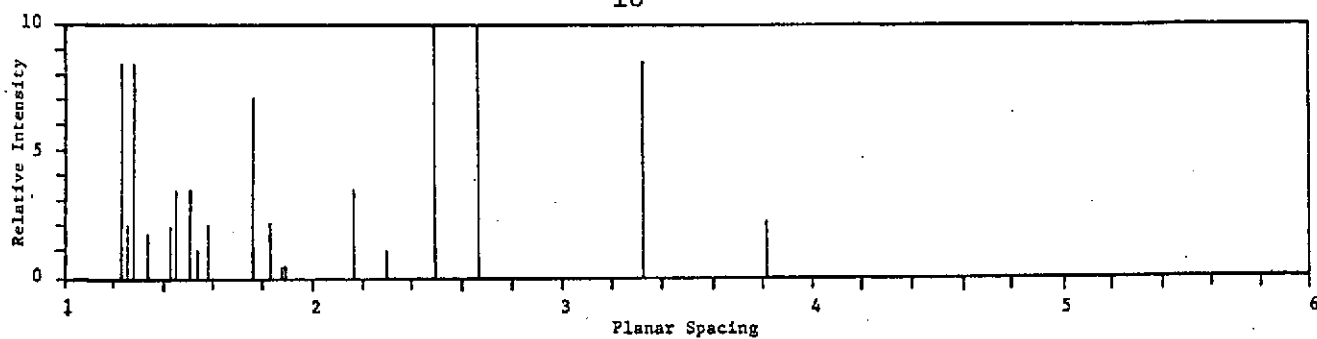
The effect of the 16-hour purification treatment on the properties of the powder was determined using Material G (Montecatini) powder. From X-ray diffraction data, it was revealed that the material had completely converted to single phase β as shown in Figure 4. This corresponds to the data of Lange⁽⁴⁾ who showed complete conversion to β following 4 hours at 1600 C.

Centrifugal sedimentation measurements of the particle size distribution revealed that the median particle size of the powder had increased during the treatment from 4.7 to 9.5 μm as shown in Figure 5. Compaction curves generated on the material in the as-received and heat-treated state, after the method of Bennett, et al⁽⁵⁾, indicated that this "powder coursening" is the result of formation of rather dense aggregates during the heat treatment. After dry ball-milling for 16 hours, the aggregates were removed from the powder.

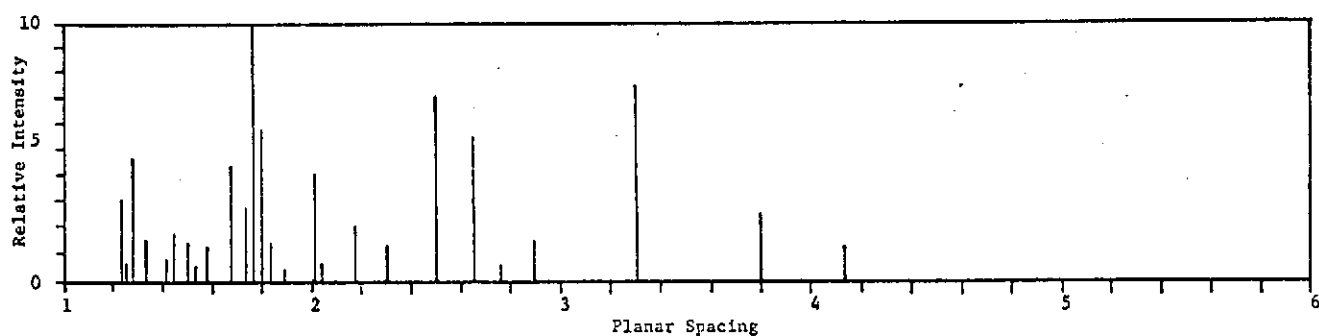
The impurity content of the powder following the heat treatment remained essentially constant with the exception of the iron content which was reduced one-half. The chemical composition of the silicon nitride was altered to values closer to stoichiometric proportions. The nitrogen content of the powder was increased to 39.69 weight percent from a starting value of 39.56 weight percent.

Summary of Treatment Results

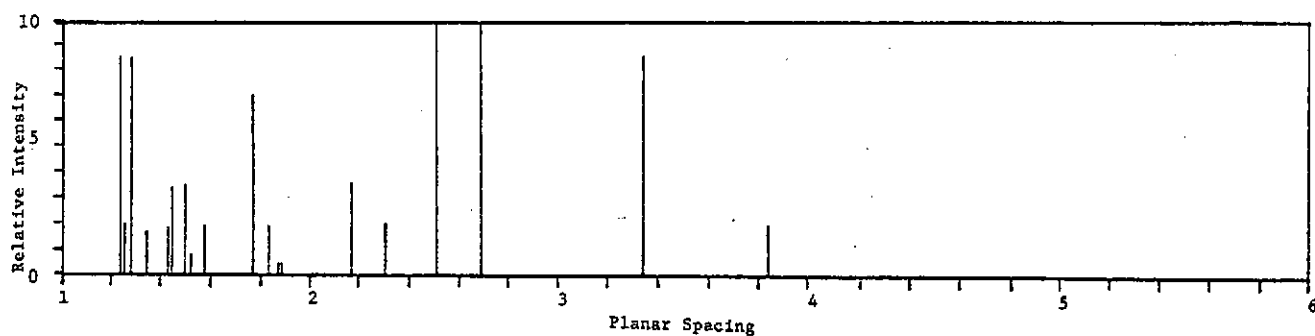
It has been shown from the preceding experiments that it is possible to achieve significant reduction in the oxygen content of silicon nitride powders through thermal treatment. Based on the experimental conditions examined, a treatment of 1600 C for 16 hours at 4×10^{-3} MN/m² (30 Torr) nitrogen overpressure yielded optimum results based on both removal rate and total oxygen removed.



(a) Powder Diffraction Pattern No. 9-259, β - Si_3N_4



(b) Type G Powder, As Received ($\sim 25\%$ α)



(c) Type G Powder, Heat Treated 16 Hours
at 1600 C Under 4×10^{-3} MN/m² (30
Torr) Nitrogen

FIGURE 4. EFFECT OF THERMAL PURIFICATION TREATMENT ON SILICON NITRIDE POWDER

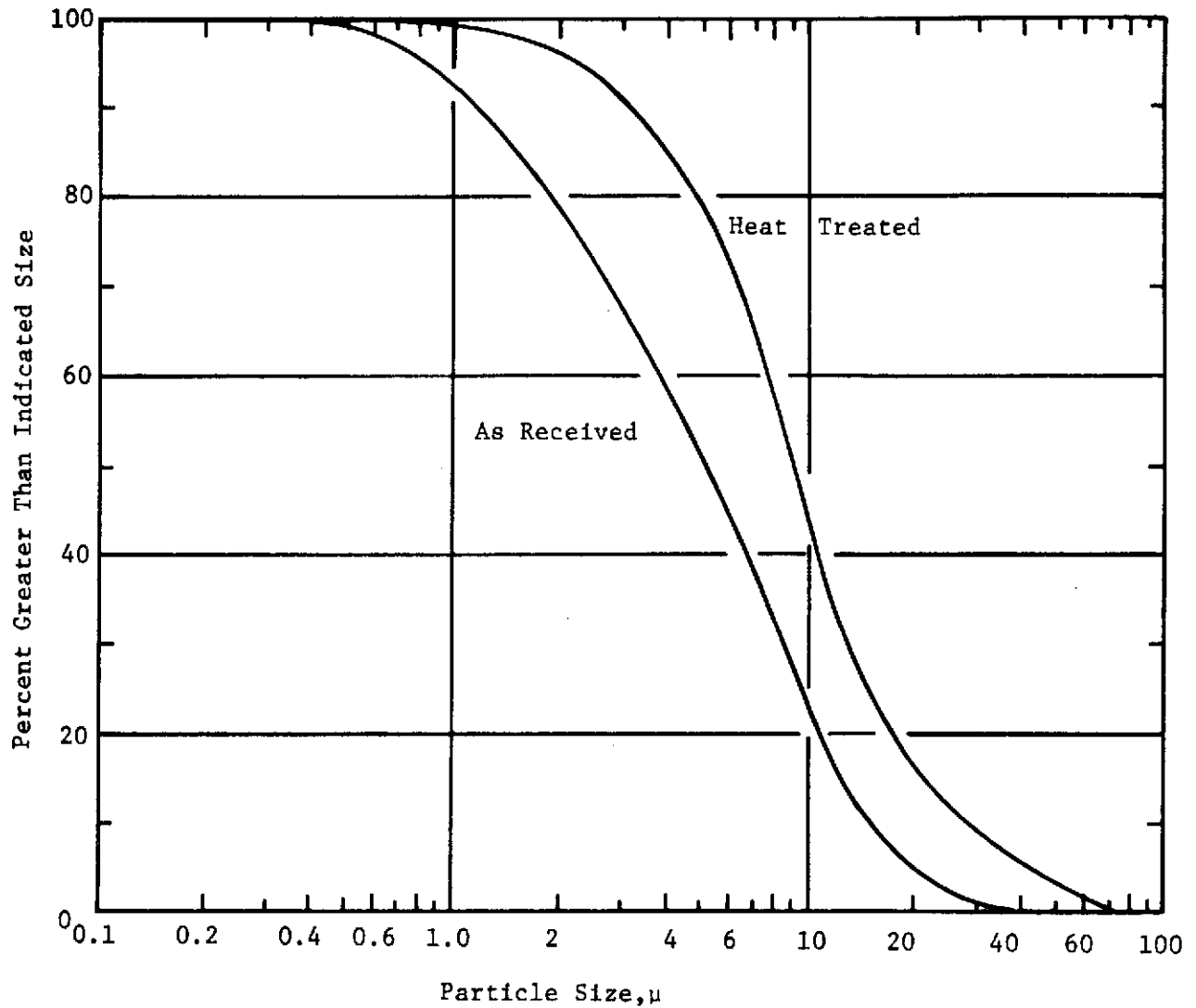


FIGURE 5. EFFECT OF HEAT TREATMENT ON PARTICLE SIZE DISTRIBUTION

Type G Powder--16 hr heat treatment at 1600 C under 4×10^{-3} MN/m² (30 Torr) nitrogen.

The resultant powder from thermal treatment was single phase β and of a slightly higher purity than the initial material. Although the effective particle size of the powder increased with the heat treatment through formation of aggregates, these could be removed by subsequent milling.

III. ADDITIVE EVALUATION

As shown in the Materials Purification Studies, approximately 50 percent of the oxygen (oxide) in the silicon nitride powder can be removed by the thermal treatment. In order to eliminate the remaining silica, it is necessary to select additives which will allow the oxide phase to be taken into solid solution in the silicon nitride crystal lattice. In addition to compensating for the residual oxygen in the system, the additive should also perform as a densification aid.

Initial selection of potential additive systems were made based on crystallographic estimations and postulation from the published literature. Basically, three additive classes were considered; oxides, nitrides, and a combination of the two.

Materials Preparation

Material F powder (Shieldalloy) was heat treated in 150 g lots at 1600 C under 4×10^{-3} MN/m² (30 Torr) nitrogen pressure. After four lots of powder were treated, all were blended together and sampled for oxygen analysis. It was determined that the residual oxygen level was 1.34 percent.

Additive amounts were calculated based on this amount and added to the silicon nitride by ball milling under inert atmosphere conditions using oxygen-free n-grade hexane as the milling liquor. Initial millings were performed in a stainless steel mill using tungsten-carbide as a media. At a later date, the mill and grinding media were changed to 99.9 percent Al₂O₃.

Hot pressing of the prepared powder blends were performed in inductively heated graphite dies under approximately 5×10^{-2} MN/m² (1/2 atm.) of nitrogen. The system was evacuated to $\sim 10^{-6}$ MN/m² ($\sim 10^{-5}$ Torr) prior to backfilling with the desired amount of nitrogen. A barrier of tantalum and graphite foils was placed between the powder and the graphite die wall.

The technique employed during hot pressing was apply a pressure of 6.9 MN/m^2 (1000 psi) to the compact prior to heating. As the compact was heated, deformation was monitored. When the compact began to deform, the pressure was increased to 34.5 MN/m^2 (5000 psi) and maintained at this level until deformation ceased. In the event that the desired amount of deformation could not be obtained, the temperature was increased (under 34.5 MN/m^2) until the desired movement was obtained. A temperature of 1750-1800 C was chosen as the maximum cutoff temperature.

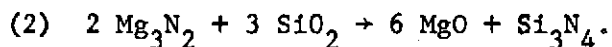
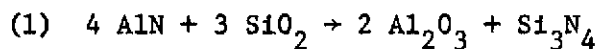
Preliminary additive evaluations at this point in the study were based on the ability of a composition to attain a high bulk density following consolidation by hot pressing. Compositions which could be densified were then evaluated with regard to the structure developed in the following program task. A discussion of each of the additive materials employed in this task follows.

Pure Silicon Nitride

The hot pressing behavior of purified, and ball milled, Material F was evaluated at 1750 C and 34.5 MN/m^2 (5000 psi) for 1, 2, and 4 hours. The chamber was evacuated to $\sim 10^{-6} \text{ MN/m}^2$ ($\sim 10^{-5}$ torr) and backfilled with $5 \times 10^{-2} \text{ MN/m}^2$ (1/2 atm.) of nitrogen. This atmosphere was maintained through the cycle. Pellets obtained were quite hard and strong; however, the maximum density obtained was only 57 percent of theoretical.

Nitride Additives

Nitride additions were made to the purified powder according to the following reactions. All oxygen was assumed to be present as SiO_2 .



Addition of the nitride materials is based upon reduction of the SiO_2 surface layer and taking the oxide product (Al_2O_3 or MgO) into solid solution

in Si_3N_4 . In this manner the strength limiting grain boundary phase should be eliminated.

The hot pressing experiments performed with the nitride additions are listed in Table 4. It should be noted that compositions designated -1 contain exact stoichiometric amounts of additive according to the reactions shown above and the amount of oxygen present in the heat treated silicon nitride powder. Specimens designated as -2 contain twice the stoichiometric amount.

In the case of aluminum nitride, attempts were also made to duplicate some of the sialon work through adding sufficient AlN to equalize the aluminum ion concentration in 20 and 35 m/o Al_2O_3 sialon's.

It was noted that the AlN did not effectively perform as a densification aid. The maximum density which could be obtained regardless of the additive content was only approximately 80 percent of theoretical.

On the other hand, the Mg_3N_2 behaved quite effectively as a densification aid. Both the stoichiometric and excessive amounts yielded structures which were near full density.

Oxide Additives

Typically $\alpha\text{-Si}_3\text{N}_4$ contains ~2 weight percent oxygen as a lattice substitute for nitrogen in addition to the silica present on the surface of the particles. Because high percentages of oxygen are apparently soluble in Si_3N_4 , an approach to eliminating oxygen from the grain boundaries would be to introduce an additive which would cause the oxygen to go into the lattice during subsequent processing.

For example, it has been shown that Al_2O_3 can be taken into solid solution in Si_3N_4 with the required charge balance being maintained by creating 1/4 of a silicon vacancy for each Al_2O_3 . The silicon vacancies will permit the grain boundary oxygen to be taken into solution.

Another additive which may give similar results is MgO . Crystal chemistry data based on ionic size criteria indicate that certain levels of MgO

TABLE 4 . SUMMARY OF NITRIDE ADDITIVE HOT-PRESSING STUDIES

Specimen Designation	Composition, weight percent			Hot-Pressing Conditions				Bulk Density, g/cm ³
				Temper- ature, C	Time, hr	Pressure		
	Si ₃ N ₄ *	Mg ₃ N ₂	AlN			MN/m ²	(psi)	
F-MN-1	97.24	2.76	-	1495 1750	1-1/2 1/2	34.5 Ditto	(5000) (Ditto)	3.163
F-MN-1	97.24	2.76	-	1500 1680	2 1	" "	(" ("))	3.175
F-MN-2	94.48	5.52	-	1500 1750	2 1/2	" "	(" ("))	3.136
F-AlN-1	97.74	-	2.26	1710	2	"	(")	2.09
F-AlN-1	97.74	-	2.26	1530 1720	1 1	" "	(" ("))	2.00
F-AlN-2	95.48	-	4.52	1710	2	"	(")	1.65
F-AlN-20	77.38	-	22.62	1550 1800	1-1/2 2	" 55.2	(" (8000))	Melted
F-AlN-20	77.38	-	22.62	1800 1800	1/4 1	6.9 34.5	(1000) (5000))	2.54
F-AlN-35	61.37	-	38.63	1550 1800	1-1/2 2	34.5 55.2	(5000) (8000))	Melted
F-AlN-35	61.37	-	38.63	1800 1800	1/4 1	6.9 34.5	(1000) (5000))	2.23

* All pressing performed with Material F having an oxygen level of 1.34 weight percent.

should be soluble in Si_3N_4 so long as an excess of cations are not available. This criteria indicates that for every MgO added to the lattice, $1/2$ an O^{-2} ion can be taken into solution through the creation of vacancies.

Using the above vacancy generation mechanisms, both Al_2O_3 and MgO were evaluated as additive materials. Based on the purified Si_3N_4 having a 1.35 weight percent oxygen content, the following compositions were formulated based on the criteria described above.

- (1) 95.88 weight percent Si_3N_4 - 4.12 percent Al_2O_3
- (2) 88.05 weight percent Si_3N_4 - 11.45 percent MgO.

Both compositions were hot pressed in tantalum-foil lined dies. The MgO containing composition was preloaded with 6.9 MN/m^2 (1000 psi) and heated slowly while the deformation was monitored. As considerable movement was encountered at 1500 C, the pressure was increased to 34.5 MN/m^2 (5000 psi). After deformation ceased, the temperature was increased to 1750 C and held until the desired degree of deformation was obtained ($\sim 1/2$ hour). The specimen exhibited a density of 3.178 g/cm^3 .

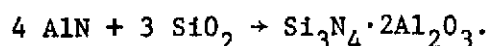
Considerable difficulty was encountered in preparing the Al_2O_3 specimens. Initially, a procedure similar to that used for the MgO additive was employed; however, the density obtained was only 2.70 g/cm^3 . The required amount of deformation was never obtained. Additional attempts were also conducted at temperatures up to 1800 C and pressures of 55.2 MN/m^2 (8000 psi). The maximum density obtained was 2.77 g/cm^3 .

From these series of hot pressing trials, it was apparent that the MgO additives were sufficient to provide composition densification. Unfortunately, the Al_2O_3 was not present in sufficient amounts to allow densification under the levels of pressure and temperature attempted.

Dual Additive Approach

Based on data of Oyama,⁽⁶⁾ Al_2O_3 additions of ~ 20 m/o are required to densify Si_3N_4 . This being the case, the oxide additions attempted in this study were obviously insufficient. In addition, it has also been reported that additions of alumina to oxygen containing Si_3N_4 will form a "J-phase", $\text{Si}_3\text{N}_4 \cdot 2\text{Al}_2\text{O}_3 \cdot \text{SiO}_2$. It was believed that this phase could possibly perform as second-phase inclusions and be strength limiting.

It was also shown that AlN would not act as a densification aid; however, the nitride should prevent "J-phase" formation through the reaction



Because the product of the $\text{AlN} + \text{SiO}_2$ reaction is Al_2O_3 in Si_3N_4 , it was believed that the material could then be densified through the addition of excess Al_2O_3 . The final product should be a solid-solution of Al_2O_3 in Si_3N_4 without damage of "J-phase" formation.

It was decided to formulate compositions from Si_3N_4 , AlN , and Al_2O_3 to form the Si_3N_4 -20 m/o Al_2O_3 as one dual-additive composition. In order to provide a variation in the final Al_2O_3 content, it was also decided to prepare a higher Al_2O_3 composition. According to Oyama, considerable grain growth occurs in compositions ≥ 40 m/o Al_2O_3 . In light of this observation, it was decided to also prepare a composition which would result in a Si_3N_4 -35 m/o Al_2O_3 final product.

Hot pressings of both materials were performed as described previously. It was observed that densification could be accomplished quite easily at 1750 C for 1 hour under 34.5 MN/m^2 (5000 psi).

On the basis of the final bulk density obtained by hot pressing, five experimental compositions were selected for further evaluation.*

* The compositions shown are based on a Si_3N_4 oxygen content of 1.35 weight percent.

- (1) Si_3N_4 - 2.76 weight percent Mg_3N_2 (MN-1)
- (2) Si_3N_4 - 5.52 weight percent Mg_3N_2 (MN-2)
- (3) Si_3N_4 - 11.95 weight percent MgO (MO-1)
- (4) Si_3N_4 - 2.06 weight percent AlN - 12.66 weight percent Al_2O_3 (20 ALON)
- (5) Si_3N_4 - 1.76 weight percent AlN - 25.20 weight percent Al_2O_3 (35 ALON).

IV. MATERIAL EXAMINATION

The five materials selected from the hot pressing study were subjected to further evaluations to provide a selection of material systems on the basis of phase analysis and structure. As all compositions were essentially full density, density in this task was not used as an examination or evaluation criteria. The evaluation techniques utilized included cursory strength measurements, X-ray diffraction, metallographic examination, and scanning electron microscopy.

Magnesium Nitride Additives

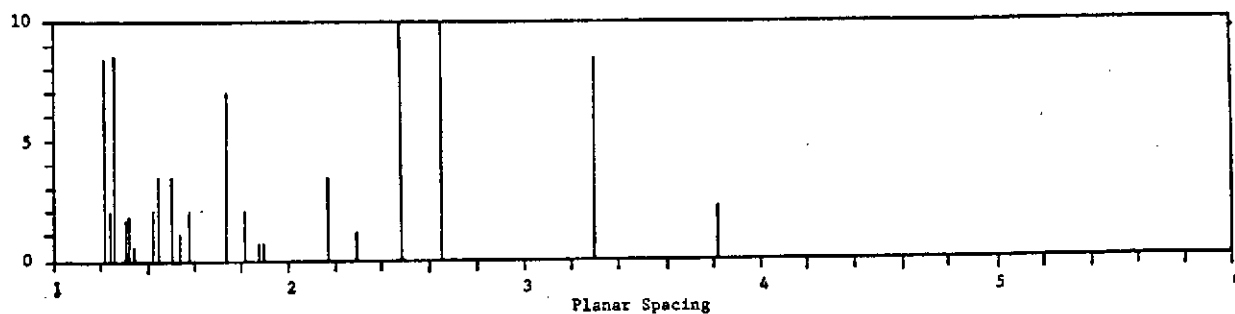
As previously stated, Mg_3N_2 additions were made to silicon nitride in two levels. The first level, Composition MN-1, was the amount required to provide a stoichiometric balance with the oxygen present in the system. The second level, Composition MN-2, was exactly twice the calculated stoichiometric level.

Both compositions appeared to be single phase according to X-ray diffraction and metallographic examination. The peak intensity chart of Composition MN-1 is shown in Figure 6 along with the standard powder diffraction pattern for β - Si_3N_4 and Si_3N_4 . It will be noted that the pattern for Composition MN-1 corresponds exactly with the standard for β - Si_3N_4 except for some changes in the peak intensity.

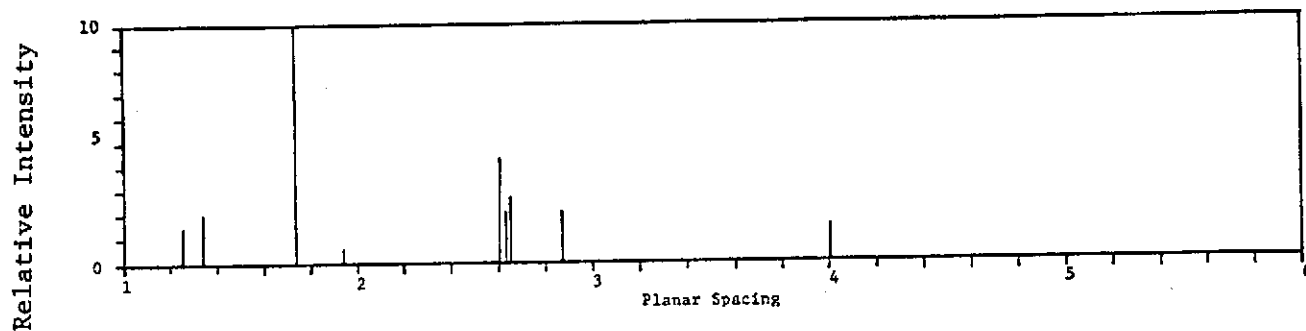
Little difference was noted in the microstructure of either composition when viewed by reflected light during metallographic examination. Both materials were extremely fine grained which led to considerable difficulty in defining the structure. Attempts at etching the structure using recommended etchants for silicon nitride* proved unsuccessful. Because the action of these etchants

* Etchants attempted were:

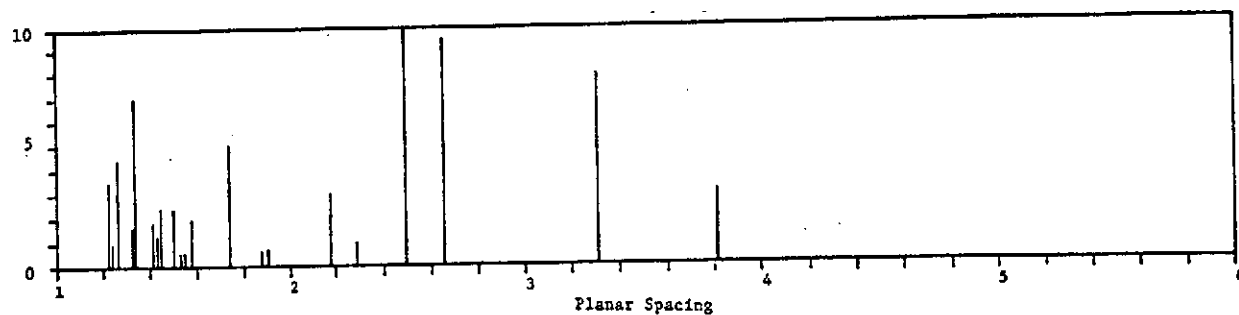
- (a) HF/ HNO_3 mixture cold
- (b) Hot phosphoric acid for various times
- (c) Molten K_2CO_3 and NaF.



(a) Powder Diffraction Pattern No. 9-259, β - Si_3N_4



(b) Powder Diffraction Pattern No. I-1289, Mg_3N_2



(c) Composition MN-1

FIGURE 6. EFFECT OF MAGNESIUM NITRIDE ADDITION ON Si_3N_4

depends on attacking the grain boundary silicate phase common to most commercial silicon nitride, failure to etch was taken as an indication of the grain boundary purity.

Examination of fracture surfaces by scanning electron microscopy revealed "clean" grain boundaries in Composites MN-1. Examination of Composition MN-2 revealed the presence of a grain-boundary phase which appears to bond the grain together. It was hypothesized that this phase could be a nitride analog of the $\text{MgO} \cdot \text{SiO}_2$ found and identified in MgO-containing silicon nitride. While no X-ray evidence was found in this study to verify the existence of such a phase, Jack ⁽⁷⁾ has prepared and identified a $(\text{Mg}, \text{Si})\text{N}$ phase. Scanning electron micrographs of both Mg_3N_2 containing specimens are shown in Figure 7. The grain boundary phase is readily apparent in Figure 7 (b) for the MN-2 composition.

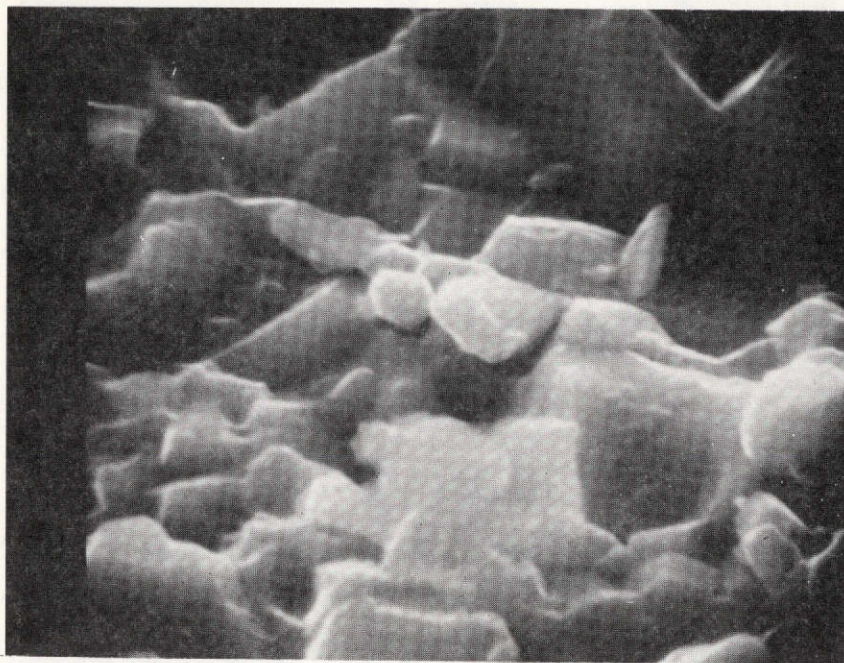
Tensile strengths, as measured by diametrical compression also reflects the presence of a brittle grain boundary phase. Composition MN-1 exhibited strengths of 463 MN/m^2 (67,200 psi) while the strength of the Composition MN-2 specimen averaged $\sim 220 \text{ MN/m}^2$ (32,000 psi).

Based on the above, Mg_3N_2 was selected as an additive material for further study with the stipulation that only a stoichiometric amount, based on the oxide content of the powders, be utilized. Hyperstoichiometric additions will lead to the formation of a grain boundary phase which weakens the structure.

Magnesium Oxide Additives

Metallographic examination of Composition MO-1 revealed the presence of a second phase which was confirmed as being MgO by X-ray diffraction. The microstructure of the composition is shown in Figure 8. Attempts were made to homogenize the structure by heat treating samples at 1700 C for various periods of time. Except for removing MgO from the surface of the specimen by vaporization, the structure was unaffected by the heat treatment. Although crystal chemistry criteria were satisfied according to theory, the solubility limit for MgO in the Si_3N_4 structure was obviously exceeded. For an extremely low starting oxygen

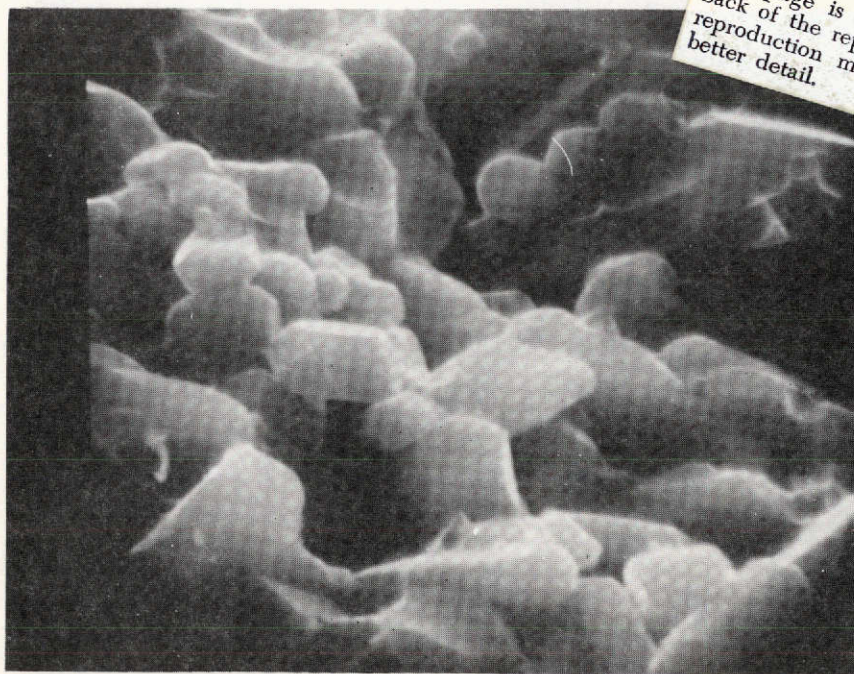
REPRODUCIBILITY OF THE
ORIGINAL PAGE IS POOR



10,000X

S12698

(a) Composition MN-1



10,000X

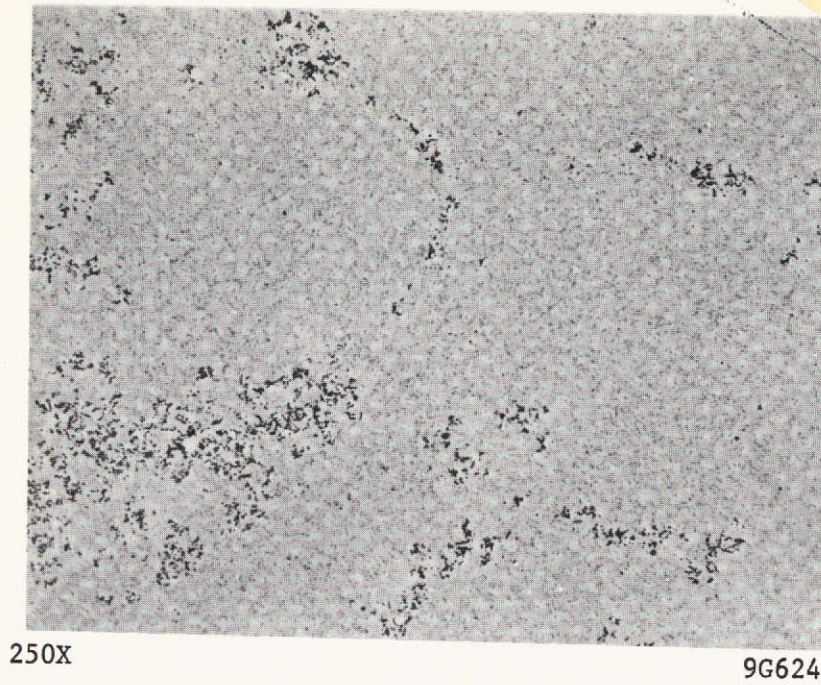
S12684

(b) Composition MN-2

This page is reproduced at the
back of the report by a different
reproduction method to provide
better detail.

FIGURE 7. FRACTURE SURFACE OF Si_3N_4 CONTAINING Mg_3N_2 ADDITIVE

REPRODUCIBILITY OF THE
ORIGINAL PAGE IS POOR



This page is reproduced at the
back of the report by a different
reproduction method to provide
better detail.

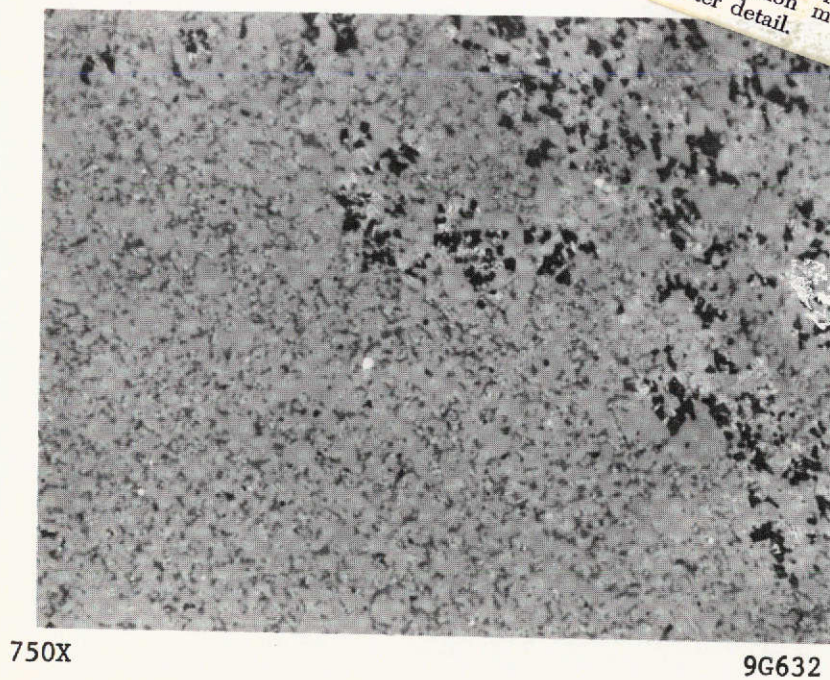


FIGURE 8. COMPOSITION MO-1 MICROSTRUCTURES

Note two-phase structure consisting
of MgO and Si_3N_4

content Si_3N_4 powder, the concept still may be feasible; however, based on the observation at this point, the composition was dropped from further consideration. It should be mentioned that the tensile strength, as measured by diametrical compression was fairly high as values of $\sim 413 \text{ MN/m}^2$ (60,000 psi) were recorded.

Dual Additive Materials

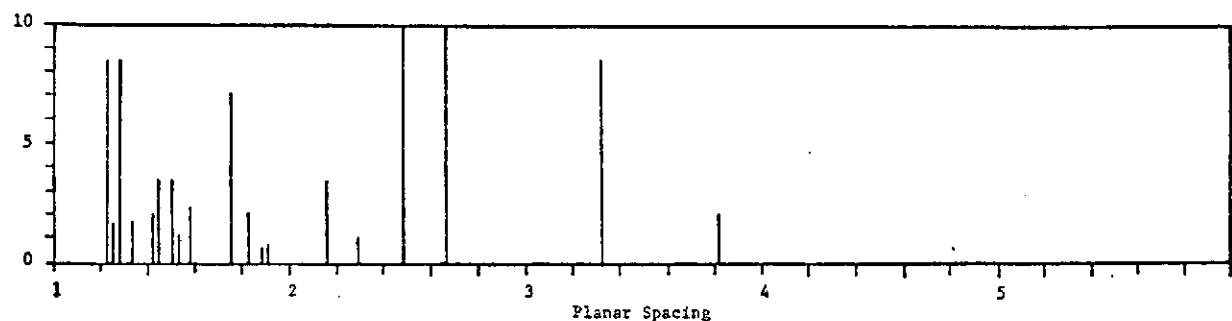
Compositions 20 AlON and 35 AlON were found to be essentially single phase by both metallographic and X-ray examinations. This is to be expected according to the tentative phase design of Oyama⁽⁸⁾ which shows solid solubility of Al_2O_3 in Si_3N_4 of up to ~ 70 mole percent. The X-ray diffraction pattern for Composition 20 AlON is shown in Figure 9(e). Standard patterns are shown for $\beta\text{-Si}_3\text{N}_4$, $\alpha\text{-Al}_2\text{O}_3$, and AlN.

It is interesting to note that the pattern for 20 AlON closely resembles that of $\beta\text{-Si}_3\text{N}_4$ with some line shifting and splitting reflecting the formation of $\beta'\text{-Si}_3\text{N}_4$ which is an expanded β structure. No traces of the AlN oxide compensation additive are apparent.

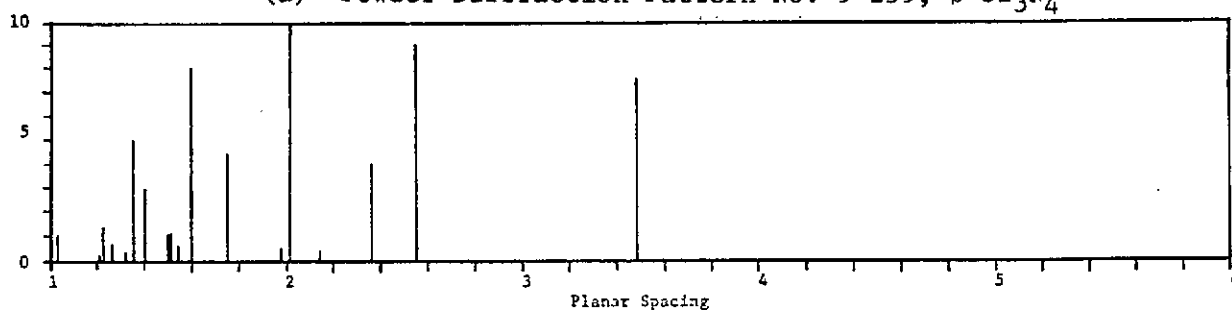
Comparing pattern (d) with (a) and (e) illustrates the effect of the AlN addition on the structure. The appearance of several additional lines in pattern (d) may be indicative of the appearance of the previously alluded to "J" phase.

The microstructure of the 20AlON composition is shown in Figure 10. The grain boundaries were found to be quite clear as observed by SEM examination of fractured surfaces and the failure of the material to be attacked by chemical etchants.

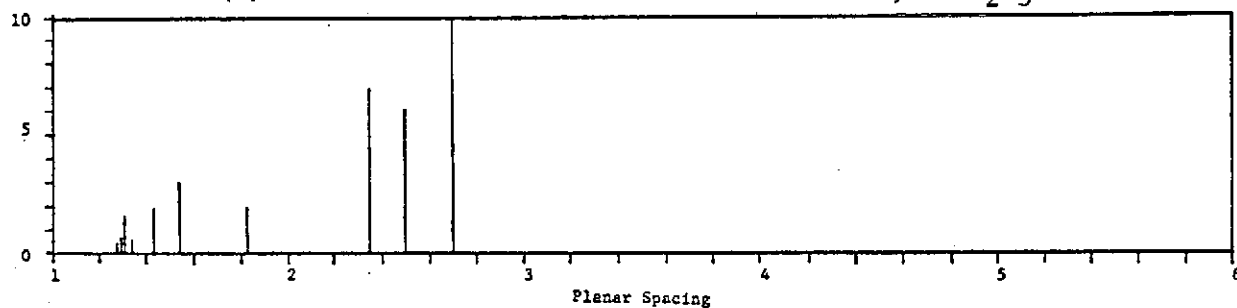
The tensile strength, as measured by diametrial compression, was relatively low, 275 MN/m^2 (40,000 psi), as compared to some of the other materials. Based on the grain structure shown in Figure 10, this was believed due to powder treatment or incomplete milling. Because of the "clean" nature of the grain



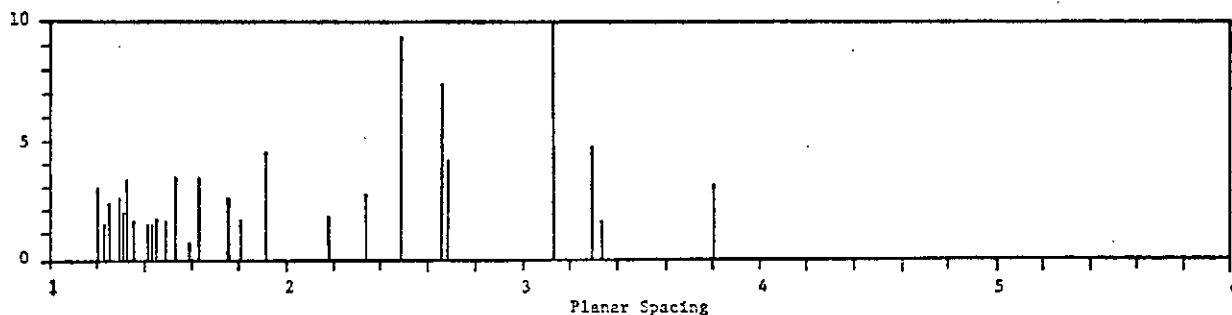
(a) Powder Diffraction Pattern No. 9-259, β - Si_3N_4



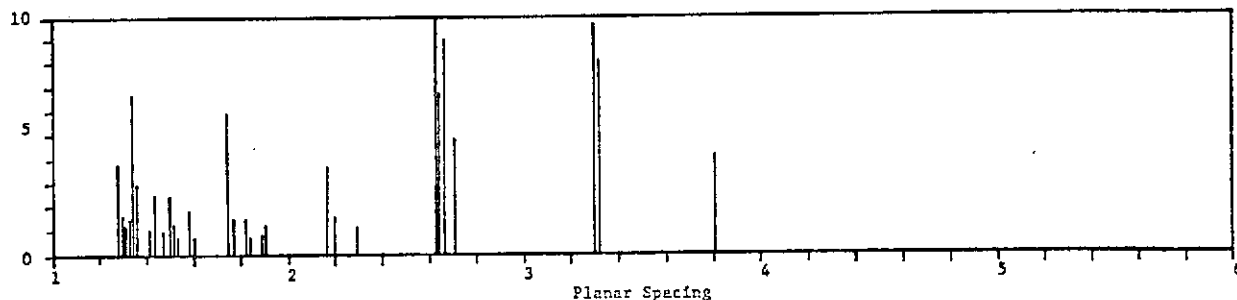
(b) Powder Diffraction Pattern No. 10-173, α - Al_2O_3



(c) Powder Diffraction Pattern No. 8-262, AlN



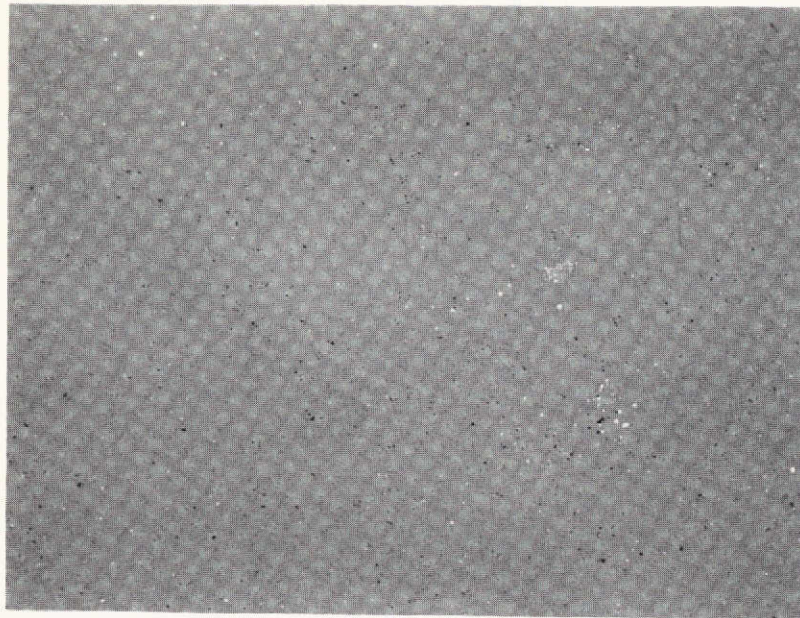
(d) Hot-Pressed Sample $\text{Si}_3\text{N}_4 + 20 \text{ m/o } \text{Al}_2\text{O}_3$



(e) Sample 20A10N

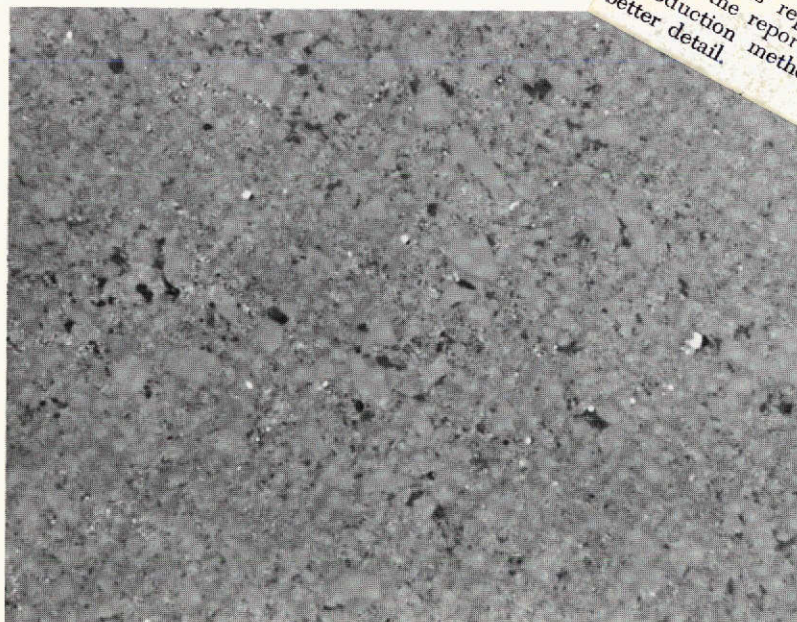
FIGURE 9. DUAL ADDITIVE SIALON, COMPOSITION 20A10N

REPRODUCIBILITY OF THE
ORIGINAL PAGE IS POOR



250X

9G628



750X

9G631

This page is reproduced at the
back of the report by a different
reproduction method to provide
better detail.

FIGURE 10 . COMPOSITION 20-A10N PREPARED FROM MATERIAL F

boundaries and the X-ray results, both Composition 20 AlON and 35 AlON were selected for further study.

Based on the results of the hot-pressing studies and the examinations performed, three compositions were selected for further study:

(1) MN-1 (Mg_3N_2 ~ stoichiometric additive)

(2) 20 AlON ($\text{AlN} + \text{Al}_2\text{O}_3$ additive)

(3) 35 AlON ($\text{AlN} + \text{Al}_2\text{O}_3$ additive).

V. TEST BILLET CONSOLIDATION

The objective of this task was to prepare test billets from the selected materials which could be machined into specimens for impact testing.

Fifteen pounds of Material F (Shieldalloy) were processed for billet fabrication. Upon receipt of the material, it was noted that the material quality was considerably lower than that received and utilized in the initial study. While the initial material was a creamy white color, the second shipment was a dark gray. The basic difference in the material was in the oxygen content. The material procured for billet fabrication exhibited an oxygen content of 3.84% along with a considerable amount of free silicon metal. Following heat treatment at 1600 C for 16 hours under 4×10^{-3} MN/m² (30 Torr) of nitrogen, the oxygen content could only be reduced to 3.76%. Very little free silicon remained following the heat treatment; however, the powder was severely agglomerated.

After the material was heat treated and compositions calculated based on the oxygen content, blends of the desired compositions were prepared by ball milling the proportioned components for 15 hours in an alumina mill using alumina balls. Oxygen free n-grade hexane was utilized as the milling liquor. Blending, milling, and drying were performed under an inert atmosphere.

The ball milled blends were hot pressed in tantalum foil-lined graphite dies. Two types of billets were prepared: (1) 8.9 x 6.4 x 1-cm (3.5 x 2.5 x 0.40-in.) rectangular shapes, and (2) 7.6-cm diameter x 1-cm thick (3-in. diameter x 0.40-in.) thick cylindrical shapes.

The Mg₃N₂ containing billets were pressed according to the schedule shown in Figure 11. As mentioned previously, hot pressing was performed by pressing to a desired degree of deformation. The maximum condition required to obtain near full density were 34.5 MN/m² (5000 psi) at 1750 C. The AlN + Al₂O₃ containing specimens were hot pressed according to Figure 12. Similar pressure-temperature conditions were utilized. It was noted that the time required to achieve near complete densification was much less than with the Mg₃N₂ containing test billets.

All specimens were machined by grinding with a silicon carbide wheel to the desired 0.64 x 0.64 x 5.72-cm (0.25 x 0.25 x 2.25 in.) size. All specimens

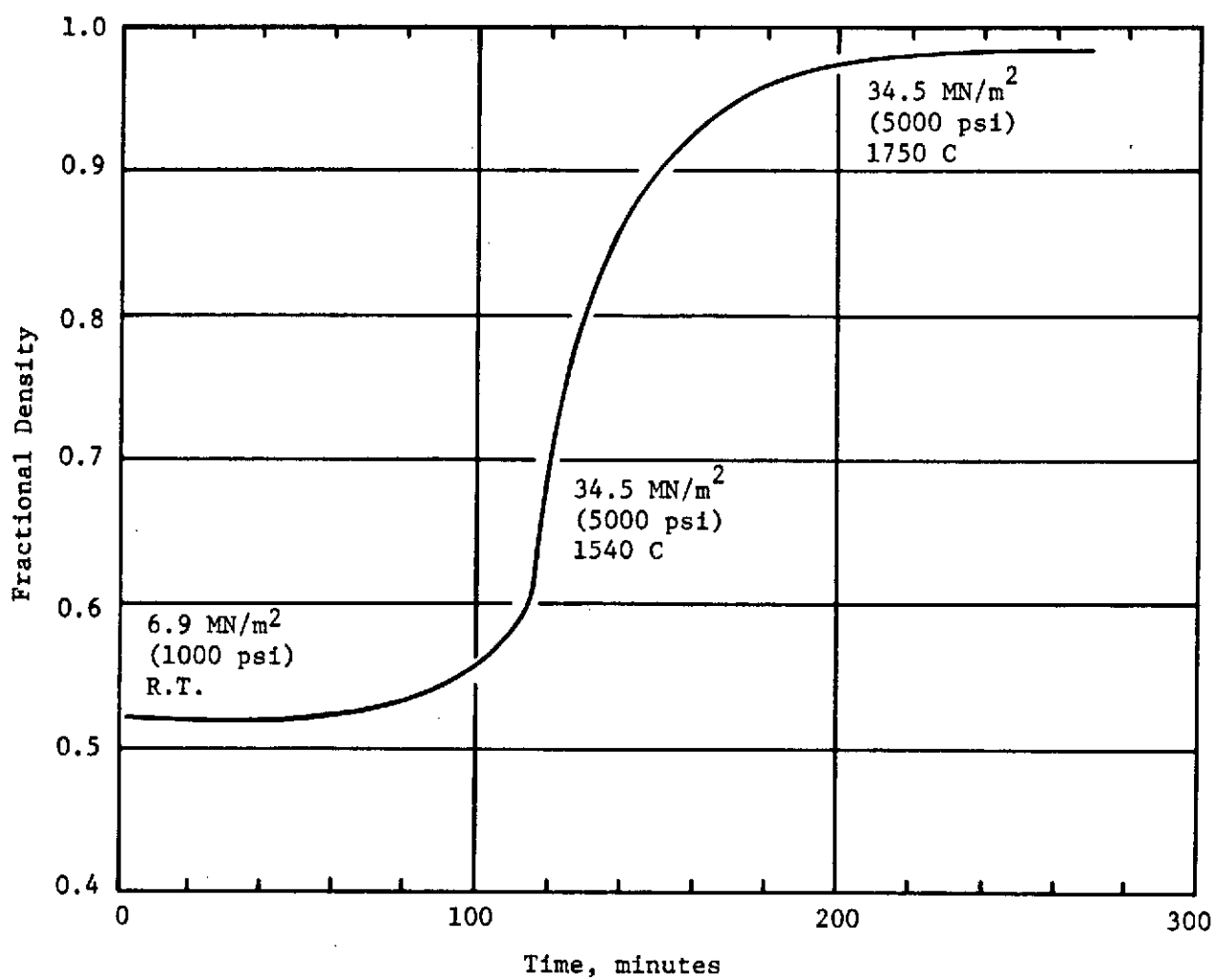


FIGURE 11. TIME-DENSITY RELATIONSHIP FOR HOT-PRESSING $\text{Si}_3\text{N}_4\text{-Mg}_3\text{N}_2$ TEST BILLETS.

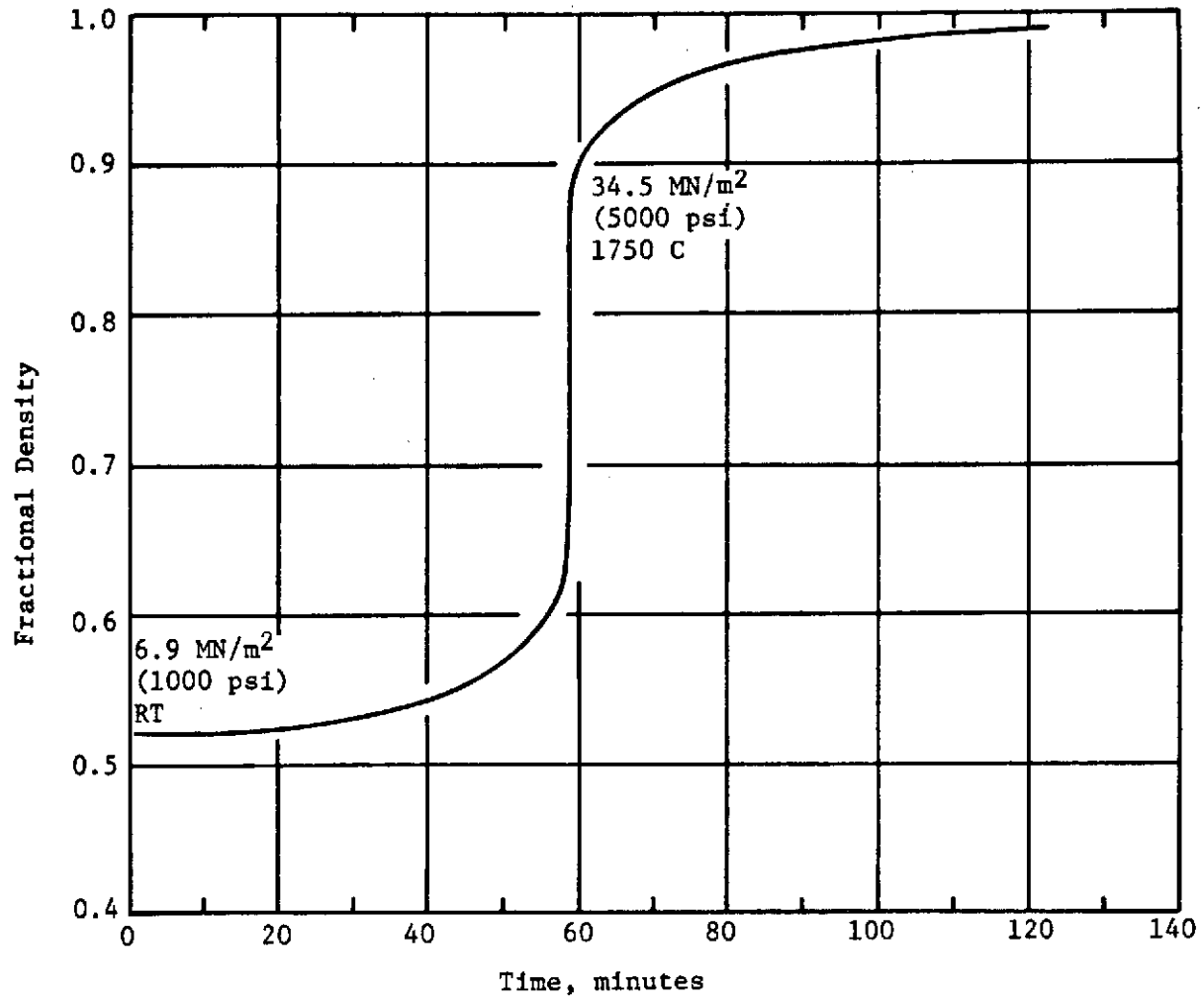


FIGURE 12. TIME-DENSITY RELATIONSHIP FOR HOT-PRESSING $\text{Si}_3\text{N}_4\text{-AlN-Al}_2\text{O}_3$ TEST BILLETS

were ultrasonically cleaned in alcohol, after which the density of the individual test bars was measured by water immersion. The composition (initial and final) and average density of the test specimens are shown in Table 5 .

TABLE 5 . COMPOSITION AND DENSITY DATA
FOR INITIAL IMPACT SPECIMENS

	F2-MN-1	F2-20AlON	F2-35AlON
Initial Composition, * weight percent	$\text{Si}_3\text{N}_4 = 92.67$ $\text{Mg}_3\text{N}_2 = 7.33$	$\text{Si}_3\text{N}_4 = 85.96$ $\text{AlN} = 5.33$ $\text{Al}_2\text{O}_3 = 8.51$	$\text{Si}_3\text{N}_4 = 73.02$ $\text{AlN} = 4.09$ $\text{Al}_2\text{O}_3 = 22.29$
Final Composition, weight percent	$\text{Si}_3\text{N}_4 = 92.12$ $\text{MgO} = 7.88$	$\text{Si}_3\text{N}_4 = 84.62$ $\text{Al}_2\text{O}_3 = 15.38$	$\text{Si}_3\text{N}_4 = 71.87$ $\text{Al}_2\text{O}_3 = 28.13$
Average Density, g/cm^3	3.163	3.061	3.078
Percent Theoretical Density	99.3	96.1	96.7

* Initial Si_3N_4 oxygen content = 3.76 percent.

VI. INITIAL TESTING

Impact Tests

The objective of this task was to measure the impact strength of specimens ground from the billets prepared in the preceding task. Charpy impact tests were performed in triplicate at room temperature, 1100, 1200, and 1325 C (2010, 2192, and 2415 F). The impact specimens were without notches and measured 0.64 x 0.64 x 5.72-cm (0.25 x 0.25 x 2.25 in). The unsupported gage length was 3.91 cm (1.54 in). It was noted that the surface quality of the ground test specimens was quite poor. The surface finish was 60 rms and numerous edge chips were present.

Testing was performed on a Physmet Impact Testing Machine (Model CIM-24) with a total capacity of 32.6 j (24 ft-lb). The dial face is graduated in degrees and is equipped with a vernier to permit accurate reading of the impact values.

Elevated temperature tests were performed by heating the specimens in air to ± 10 C over the desired temperature. Specimens were individually extracted from the furnaces and immediately tested. Thermocouple equipped control specimens indicated that the temperature at input was the desired test temperatures. The maximum, minimum, and average values recorded are listed in Table 6.

Additional Tests

Selected bars were utilized to determine the flexure strength in 4-point bend. Strain gages were attached to one specimen of each composition and the elastic modulus determined. The compositions, densities, and mechanical properties are listed in Table 7.

TABLE 6 . INITIAL IMPACT TEST RESULTS

Code (Initial Composition)	Average Density, g/cm ³	Measured Impact Strength at Indicated Temperature, J (in-lb)			
		Room Temperature	1100 C	1200 C	1325 C
F2-MN1 (Si ₃ N ₄ = 92.96%) (Mg ₃ N ₂ = 7.33%)	3.163	Max. 0.23 (2.02) Min. 0.16 (1.38) Ave. 0.20 (1.81)	Max. 0.20 (1.78) Min. 0.07 (0.66) Ave. 0.15 (1.35)	Max. 0.17 (1.54) Min. 0.15 (1.34) Ave. 0.16 (1.46)	Max. 0.19 (1.72) Min. 0.12 (1.07) Ave. 0.16 (1.45)
F2-20AlON (Si ₃ N ₄ = 85.96) (AlN = 5.33) (Al ₂ O ₃ = 8.51)	3.061	Max. 0.27 (2.41) Min. 0.14 (1.20) Ave. 0.22 (1.93)	Max. 0.15 (1.34) Min. 0.13 (1.14) Ave. 0.14 (1.28)	Max. 0.23 (2.02) Min. 0.19 (1.72) Ave. 0.22 (1.94)	Max. 0.64 (5.70) Min. 0.42 (3.74) Ave. 0.53 (4.72)
F2-35AlON Si ₃ N ₄ = 73.02 AlN = 4.69 Al ₂ O ₃ = 22.29	3.078	Max. 0.13 (1.14) Min. 0.12 (1.08) Ave. 0.13 (1.12)	Max. 0.47 (4.14) Min. 0.13 (1.14) Ave. 0.30 (2.68)	Max. 0.14 (1.20) Min. 0.12 (1.03) Ave. 0.13 (1.14)	Max. 0.16 (1.42) Min. 0.12 (1.07) Ave. 0.14 (1.25)

Note: 1 J = 8.8235 in-lb.

TABLE 7 . COMPOSITION AND SELECTED PROPERTY
DATA FOR INITIAL IMPACT SPECIMENS

	F2-MN-1	F2-20AlON	F2-35AlON
Initial Composition, weight percent *	$\text{Si}_3\text{N}_4 = 92.67$ $\text{Mg}_3\text{N}_2 = 7.33$	$\text{Si}_3\text{N}_4 = 85.96$ $\text{AlN} = 5.33$ $\text{Al}_2\text{O}_3 = 8.51$	$\text{Si}_3\text{N}_4 = 73.02$ $\text{AlN} = 4.69$ $\text{Al}_2\text{O}_3 = 22.29$
Average Density, g/cm^3	3.163	3.061	3.078
Percent Theoretical Density	99.3	96.1	96.7
Flexure Strength, MN/m^2 (psi)	256 (37,125)	285 (41,300)	245 (35,525)
Elastic Modulus, MN/m^2 (psi)	0.28×10^6 (40.2×10^6)	0.27×10^6 (39.6×10^6)	0.24×10^6 (35.2×10^6)

* Initial Si_3N_4 oxygen content = 3.76 percent.

The mechanical properties (flexure strength) were rather disappointing; however, the values were not believed to be inherent to the material. The surface quality of the specimens was quite poor with considerable edge chipping. It was believed that the specimen surfaces were subjected to considerable damage during grinding. As a result, strength values were approximately only one-half of their potential value.

As is apparent, the impact values recorded were considerably below the 0.68 j (6 in-lb) specification with the exception of the F2-20AlON specimens tested at 1325 C. The surfaces and edges of this group of specimens were diamond lapped prior to testing and therefore did not reflect the effect of surface damage on toughness as did the remainder of the specimens.

Because of these observations, it was not believed that the tests performed were a true evaluation of the toughness of the materials developed. Analysis of the impact test results and the samples indicate that the low values may be the result of

- (1) The exceptionally high oxygen content in the purified Si_3N_4 which necessitated the use of large amounts of nitride additive. The thought here is that the large amount of nitride additive could have led to strength limiting flaws.
- (2) The poor machining quality of the impact bars. Edge chipping and surface grinding marks were apparent on all specimens. It was believed that this could have reduced the flexure strength as much as 50 percent. The impact strength would have been similarly effected.

Based on the above, it was decided that the impact specimens should be refabricated from low oxygen Si_3N_4 and ground in such a manner as to obtain optimum surface conditions.

VII. BILLET REFINEMENT

The object of this task was to attempt certain processing refinements which were deemed necessary to improve the toughness of the compositions developed. The main refinement attempted were those previously listed dealing with the oxygen level of the starting powder and machining of the test specimens.

Material G powder (Montecatini-Edison) containing 0.46 weight percent oxygen was obtained and heat treated 16 hours at 1600 C under 30 Torr of nitrogen. Approximately, three pounds of powder were heat treated in 150 g lots. The lots were blended and sampled for oxygen analysis. The results of the triplicate analysis were identical at 0.24 weight percent. The nitrogen analysis of the heat treated powder was 39.69 percent.

The compositions listed in Table 8 were prepared using Mg_3N_2 powder and $3.5 \mu\text{m } \alpha\text{-Al}_2\text{O}_3$. Blends were prepared by ball milling in a high-purity alumina mill with high-purity alumina balls. Oxygen-free n-grade hexane was used as the milling liquor. All blending, milling, and drying were performed under an inert atmosphere.

Hot pressings were performed as previously described using tantalum-foil-lined graphite dies. The Mg_3N_2 containing specimens were hot pressed at 1750 C for ~4 hours under 34.5 MN/m^2 (5,000 psi). It was noted that deformation was quite slow due to the extremely small amount of Mg_3N_2 added to the blend which required a lengthening of the hot-pressing cycle. Both Al_2O_3 and AlN containing compositions were consolidated at 1750 C for 1-1/2 hours under 34.5 MN/m^2 (5000 psi) with little or no difficulty. Densities are also shown in Table 8.

Certain visible changes were observed in the material hot pressed from the low-oxygen powder as compared to that prepared from the Material F powder. The specimens prepared from Material G were light beige in color while those prepared from the high-oxygen material (F) were basically a dark gray.

TABLE 8. REFINED COMPOSITIONS FOR SECOND IMPACT TESTS

	G-MN-1	G-20AlON	G-35AlON
Initial Composition, w/o*	$\text{Si}_3\text{N}_4 = 99.5$ $\text{Mg}_3\text{N}_2 = 0.5$	$\text{Si}_3\text{N}_4 = 84.7$ $\text{AlN} = 0.35$ $\text{Al}_2\text{O}_3 = 14.95$	$\text{Si}_3\text{N}_4 = 71.94$ $\text{AlN} = 0.30$ $\text{Al}_2\text{O}_3 = 27.76$
Final Composition, w/o	$\text{Si}_3\text{N}_4 = 99.4$ $\text{MgO} = 0.60$	$\text{Si}_3\text{N}_4 = 84.62$ $\text{Al}_2\text{O}_3 = 15.38$	$\text{Si}_3\text{N}_4 = 71.87$ $\text{Al}_2\text{O}_3 = 28.12$
Average Density, g/cm ³	3.109 (~ 95%)	3.150 (~ 98%)	3.243 (~ 98%)
Percent Theoretical Density	~ 94	~ 98	~ 98

* Initial Si_3N_4 oxygen content = 0.24 percent.

"White spots", or small clusters of very fine porosity were apparent in some areas of ground specimens prepared from Material F. These have been shown to be the result of hard powder aggregates in the powder which were not removed by the milling operation.(9) It will be recalled that this powder exhibited a tendency toward agglomeration during the thermal treatment due to the high oxygen (silica) content of the powder. These "white spots", which perform as crack initiation sites, were not observed in samples prepared from Material G. This probably indicates that more effective milling and blending of the compositions was obtained during the processing of Material G samples.

Specimen machining was accomplished by slow rough grinding. After the samples were blanked from the billets, the material removal rate was reduced to ~ 0.0005 cm per pass to reduce the surface damage. Rough machining was completed at ~ 0.025 cm oversize on all dimensions after which the specimens were final ground to size (0.64 x 0.64 x 5.72 cm) using a fine diamond wheel with the same 0.0005 cm per pass removal rate. The surface finish on all specimens was 14 rms.

VIII. FINAL IMPACT TESTING

Impact testing of the refined specimens prepared in Task VII were tested in the facilities of the Avco Corporation, Systems Division, in Lowell, Massachusetts. The testing fixture, described in NASA CR-72794⁽¹⁰⁾, consists of a Bell Telephone Laboratories impact tester modified to provide impact strength data at temperatures from room to 1325 C (2415 F). The specimens are tested in the Charpy test mode using 2.71 j (2 ft-lb) hammer and a 3.99-cm (1.574-in.) gage length.

During testing, the specimens are mounted in a split furnace which utilizes SiC heater rods. The furnace closure consists of a firebrick lid and two end plugs. When the furnace achieves the desired testing temperature, the lid and end plugs are removed, the Charpy hammer released, and the impact energy recorded on a dial. The time between removal of the lid and end plugs is quite short; therefore, specimen cooling is of no consequence. The anvils for the test specimens are composed of SiC.

Impact values, as reported by Avco, are listed in Table 9 .

IX. LARGE SPECIMEN IMPACT TESTS

According to the overall program objectives or plans, unnotched Charpy impact tests were to be performed in triplicate with larger specimens on materials meeting the 0.68 joule (6 in-lb) requirement with the smaller impact bars. These tests were to utilize specimens 1.0 x 1.0 x 5.72-cm (0.4 x 0.4 x 2.25-in) and be tested with an unsupported gage length of 3.81 cm (1.50 in). Although none of the smaller bar specimens exceeded impact values greater than the 0.68 joule requirement, it was requested that the impact strength of the G-20 AlON composition be measured for the larger Charpy bars.

To comply with this request, an extra billet of G-20 AlON material was prepared by the process and techniques previously described and ground into

TABLE 9. FINAL IMPACT STRENGTHS

Code	Composition,* weight percent	Average Density, g/cm ³	Impact Strength at Temperature, J (in-lb)			
			Room Temperature	1100 C	1200 C	1325 C
G-MN-1	Si ₃ N ₄ + 0.5 Mg ₃ N ₂	3.109 (~ 94% T.D.)	Max. = 0.1890 (1.668) Min = 0.1609 (1.420) Ave = 0.1773 (1.565)	Max = 0.2155 (1.902) Min = 0.1602 (1.414) Ave = 0.1833 (1.618)	Max = 0.1944 (1.716) Min = 0.1722 (1.520) Ave = 0.1842 (1.626)	Max = 0.2379 (2.100) Min = 0.1790 (1.580) Ave = 0.1944 (1.760)
G-20A1ON	Si ₃ N ₄ + 0.35 AlN + 14.95 Al ₂ O ₃	3.150 (~ 98% T.D.)	Max = 0.2357 (2.080) Min = 0.1264 (1.116) Ave = 0.1810 (1.598)	Max = 0.1860 (1.642) Min = 0.1813 (1.600) Ave = 0.1836 (1.621)	Max = 0.3887 (3.431) Min = 0.2633 (2.324) Ave = 0.3184 (2.8103)	Max = 0.2632 (2.323) Min = 0.2549 (2.250) Ave = 0.2591 (2.286)
G-35A1ON	Si ₃ N ₄ + 0.30 AlN + 27.96 Al ₂ O ₃	3.243 (~ 98% T.D.)	Max = 0.1552 (1.370) Min = 0.1278 (1.128) Ave = 0.1410 (1.245)	Max = 0.2762 (2.438) Min = 0.1602 (1.414) Ave = 0.2182 (1.926)	Max = 0.3887 (2.431) Min = 0.2137 (1.886) Ave = 0.3012 (2.658)	Max = 0.2137 (1.886) Min = 0.1310 (1.156) Ave = 0.1724 (1.521)

* Initial composition based on Material G Si₃N₄ with an oxygen content of 0.24 weight percent.

rectangular bars of the required dimensions. Again, specimens were rough ground to ~ 0.025 cm (0.010 in) oversize in all dimensions then final ground to near the required dimensions with a fine grit diamond wheel. In the case of the larger specimens, diamond grinding was terminated at ~ 0.005 cm (0.002 in) oversize and the remaining material removed by hand lapping with minus 600 grit diamond paste. All edges were radiused during the lapping operation. The surface finish of the bars following the lapping operation was measured as a 2 RMS finish.

Three bar specimens $1.0 \times 1.0 \times 5.72$ cm ($0.4 \times 0.4 \times 2.25$ in) were impact tested in the Charpy mode using the Battelle Physmet Model CIM-24 Impact Machine equipped with a 32.6 j (24 ft-lb) pendulum. This was the same apparatus used to perform the initial impact values. Due to the limited number of specimens, all testing was performed at room temperature. The results are listed in Table 10.

TABLE 10. CHARPY IMPACT VALUES FOR LARGE SPECIMENS OF G-20A10N (ROOM TEMPERATURE)

Code	Initial Composition, weight percent	Impact Strength	
		J	in-lb
G-20A10N	$\text{Si}_3\text{N}_4 + 0.35 \text{ AlN} + 14.95 \text{ Al}_2\text{O}_3$	0.8430	7.44
		0.5574	4.92
		0.5031	4.44
	Average	0.6345	5.60

X. STRUCTURE CHARACTERIZATION

Upon completion of the impact testing, all compositions prepared from the Material G silicon nitride powder were characterized. This included the final impact specimen (Task VIII) and the large impact bars (Task IX).

Impurity analyses were conducted on samples broken from the room temperature impact bars by optical emission spectrography. It was noted that the impurity content was not appreciably increased over that of the starting powder listed earlier. Samples were also prepared under inert atmosphere conditions and submitted for oxygen analysis by inert gas fusion techniques. The results of these analysis are listed in Table 11.

Theoretical values of the oxygen content are listed for comparison with the analyzed values. This increase in oxygen was believed due to surface oxidation of the bar specimens during grinding.

Examination of the structures by X-ray diffraction revealed patterns nearly identical to those previously shown. The magnesium nitride containing material (G-MN-1) revealed a slightly shifted β - Si_3N_4 pattern. Both sialon materials (G-20AlON and G-35AlON) revealed a shifted β - Si_3N_4 structure with some line splitting which was believed indicative of β' - Si_3N_4 .

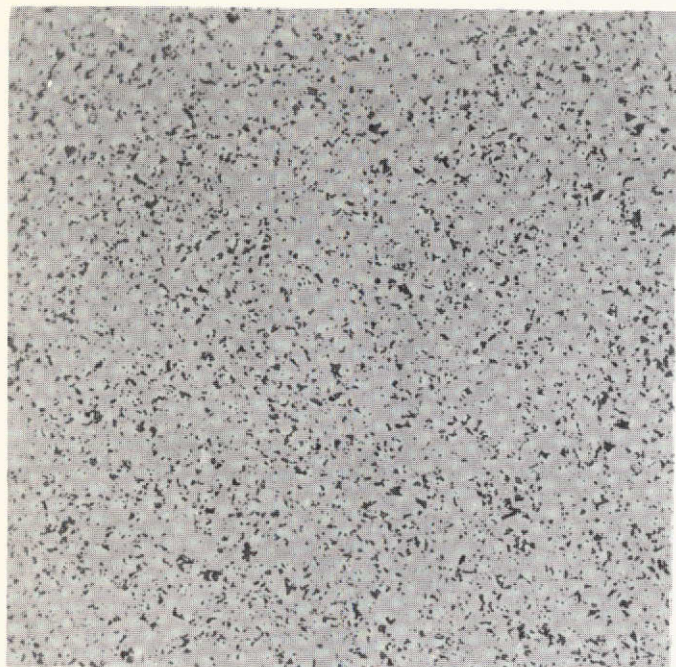
The microstructure of all three compositions was examined in three separate modes. Mounted and polished sections were examined in the as-polished condition by reflected light optical microscopy. Fractured surfaces were examined using scanning electron microscopy. Also, it was found that structure could be defined by etching in boiling phosphoric acid. Due to the ultra-fine grain size, the structure could only be examined by electron microscopy; therefore, replicas were prepared and the structure examined at 12,000X magnification. Grain size determinations were conducted using the linear intercept technique on the resultant photomicrographs.

The structure of the G-MN-1 material is shown in Figure 13. The as-polished photomicrograph indicates that the material is essentially single phase; however, as is obvious from the photomicrograph, the structure does contain a large percentage of voids. Bulk density measurement on the impact bars of this material revealed an average density of 3.109 gm/cm^3 or $\sim 94\%$ of theoretical. The as-polished photomicrograph shown in Figure 13 obviously contains more than 6% porosity. It was noted that much of the porosity shown began to develop during polishing of the specimen and is therefore assured to be a polishing artifact.

TABLE 11. IMPURITY AND OXYGEN ANALYSIS OF FINAL IMPACT BAR COMPOSITION*

	G-MN-1	G-20A10N	G-35A10N
Oxygen Analysis, weight percent (Theoretical Value)	1.45 (0.68)	8.03 (7.39)	14.16 (12.93)
Aluminum, ppm	800	-	-
Calcium, ppm	200	180	160
Iron, ppm	60	40	30
Magnesium, ppm	-	25	20
Molybdenum, ppm	<10	<10	<10
Tungsten, ppm	<50	<50	<50

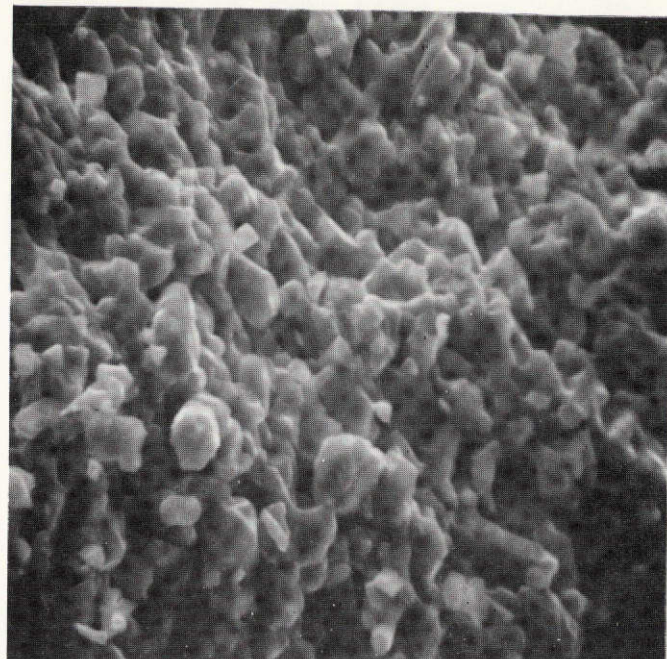
* All specimens prepared from Material G silicon nitride having an oxygen content of 0.24 percent.



250X

(a) As Polished

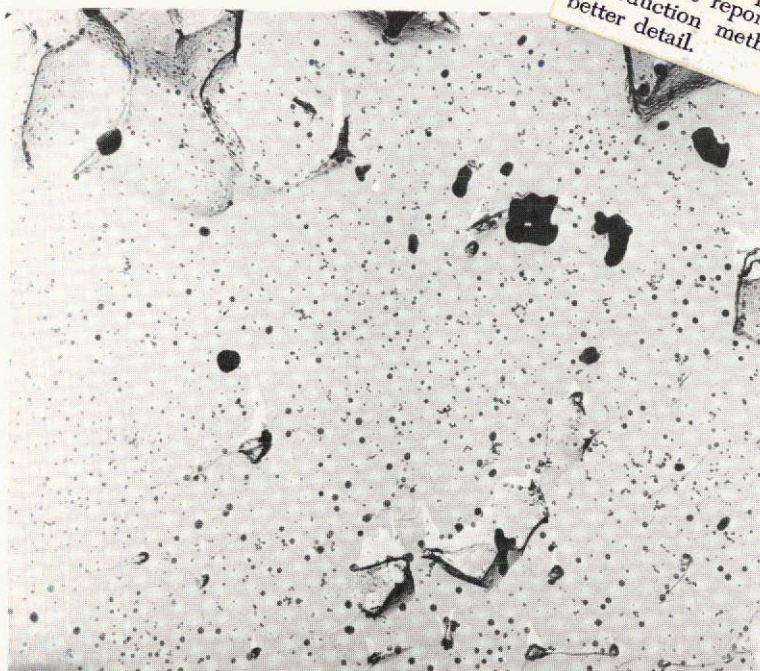
1H011



2000X

(b) Fractured Surface

S-13381



12000X

(c) Replica of Etched Surface

EH4737

This page is reproduced at the
back of the report by a different
reproduction method to provide
better detail.

FIGURE 13.

COMPOSITION G-MN-1
(99.5 w/o Si_3N_4 + 0.5 w/o Mg_3N_2)
Average Grain Size = $0.95\mu\text{m}$
Average Density = 3.109 g/cm^3

The low density for this material is apparent in the SEM view of the fractured surface which is the typical structure for a porous material. It will be noted that the fracture is intergranular. It will be recalled that the Mg_3N_2 densification aid content is a function of the oxygen content of the starting Si_3N_4 powder. Due to the extremely low oxygen level of this material, a relatively low amount of Mg_3N_2 was added. It is apparent from the structure that the amount of Mg_3N_2 utilized was insufficient to obtain full densification.

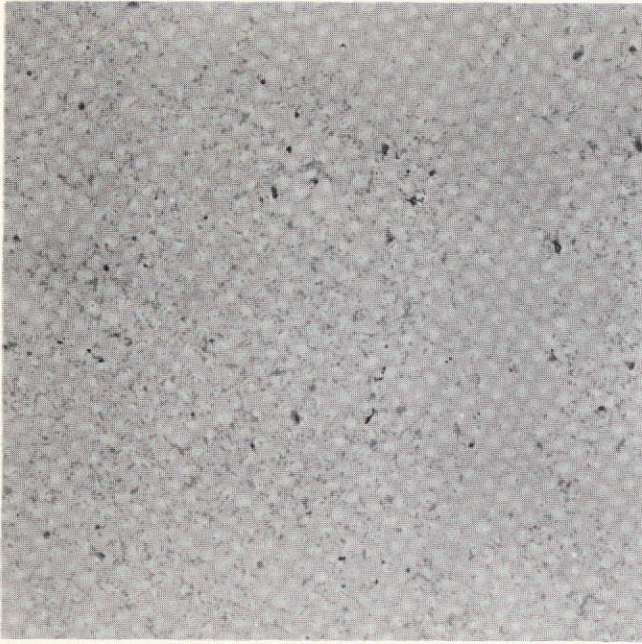
The fine structure of the Mg_3N_4 containing material can be seen in surface replica as examined by electron microscopy. Extremely faint grain boundaries may be seen in the structure. While it was not possible to analyze the grain boundary composition, it is believed that the material is MgO in solid solution with Si_3N_4 . This being the case, it appears that Mg_3N_2 can be an effective additive for compensating the grain-boundary silica.

In examining the structure, it will be noted that the pores are quite small and primarily intragranular in nature. The average grain size is $<1 \mu\text{m}$. The large dark spots and white areas are holes or raised areas in the replica surface.

The sialon materials, G-20AlON and G-35AlON, are shown in Figures 14 and 15, respectively. When examined in the as-polished condition, both materials appear to be composed of two phases with the second phase content increasing as a function of the Al_2O_3 level. This corresponds to the X-ray data which showed the samples to contain β and β' - Si_3N_4 .

The fracture surfaces of both samples indicated primarily intergranular fracture typical of high-strength, high-density, material. The preponderance of intergranular fracture was greatest in the high-alumina material, G-35AlON; however, this is believed due to the obvious difference in pore content.

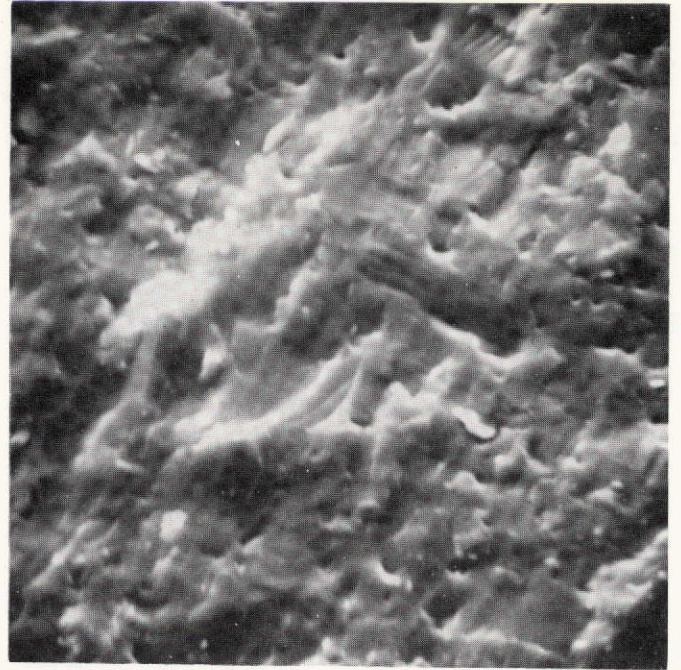
The high magnification electron microscope examination revealed very nearly the same structure for both compositions, although the increase in β' phase content is obvious in G-35AlON. The grain size of both sialon materials was approximately the same, averaging $\sim 1 \mu\text{m}$.



250X

(a) As Polished

1H013

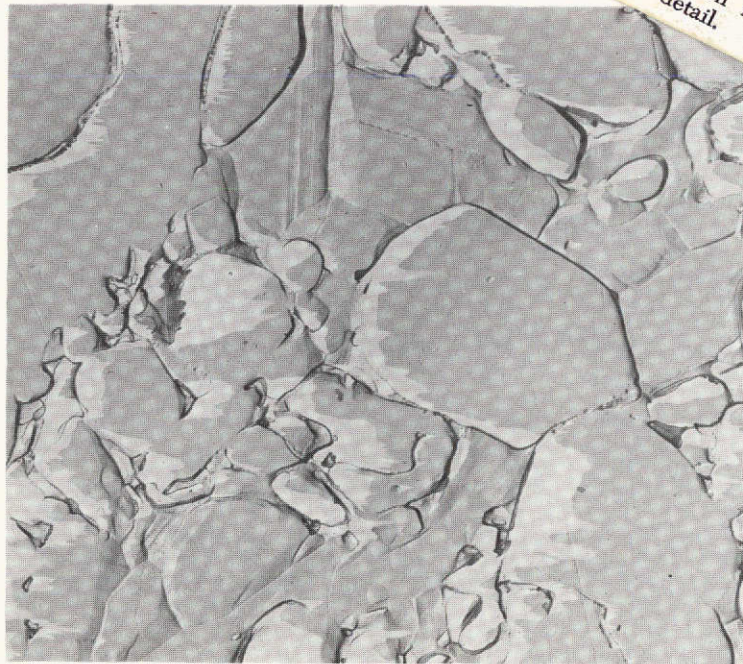


2000X

(b) Fractured Surface

S-13377

This page is reproduced at the
back of the report by a different
reproduction method to provide
better detail.



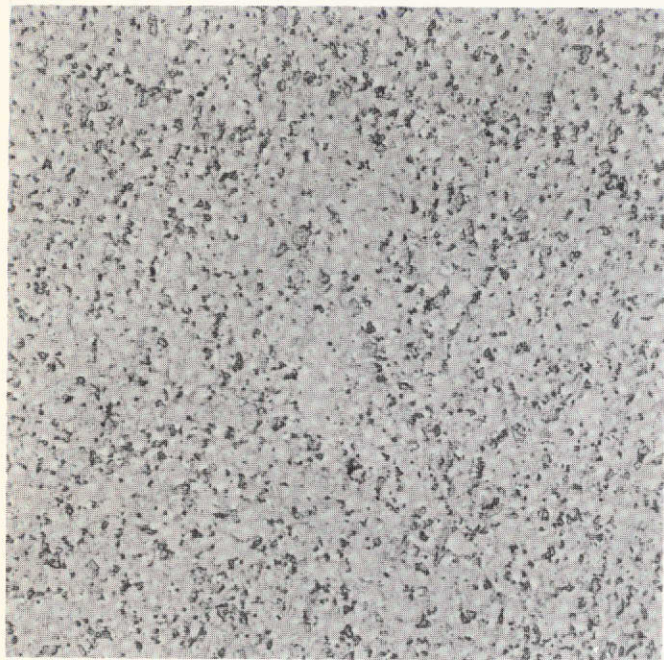
12000X

(c) Replica of Etched Surface

EH4726

FIGURE 14.

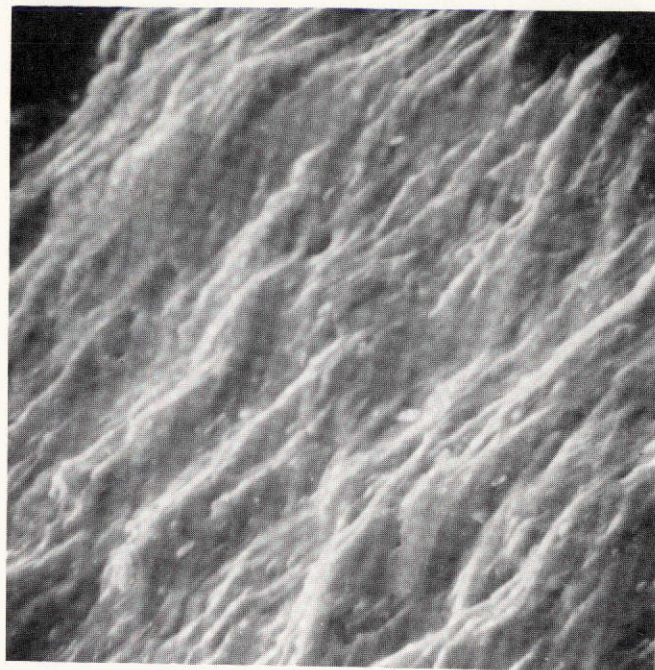
COMPOSITION G-20A10N
(84.7 w/o Si_3N_4 - 0.35 w/o AlON - 14.95 w/o Al_2O_3)
Average Grain Size = $1.02\mu\text{m}$
Average Density = 3.150 g/cm^3



250X

(a) As Polished

1H014



2000X

(b) Fractured Surface

S-13379

This page is reproduced at the
back of the report by a different
reproduction method to provide
better detail.



12,000X

(c) Replica of Etched Surface

EH4728

FIGURE 15.

COMPOSITION G-35A10N
(71.94 w/o Si_3N_4 + 0.30 AlN + 27.76 w/o Al_2O_3)
Average Grain Size = $1.00\mu\text{m}$
Average Density = 3.243 g/cm^3

While grain boundaries are readily apparent in the structure, these boundaries are not believed to contain a silicate phase as shown by the selective etching experiments. It is believed that the boundaries are composed of a different sialon composition (approximately Si_3N_4 -67 weight percent Al_2O_3) than the bulk of the material. The grain boundary phase composition is estimated from the SiO_2 -AlN reaction product composition.

XI. ADDITIONAL PROPERTY STUDIES

Although not required contractually, selected mechanical property tests were performed on samples of G-MN-1, 20-AlON, and 35-AlON to determine the effect of elevated temperatures on the mechanical response of the materials. It was believed that the absences of a silicate phase in the grain boundaries should exhibit a pronounced effect on the high-temperature behavior.

The remaining pieces of the billets from which the impact bars were ground were sectioned into specimens $0.64 \times 0.32 \times 4.45$ cm ($0.25 \times 0.125 \times 1.75$ in.) for flexure testing and into right circular cylinders 0.43 cm diameter \times 0.86 cm long (0.17 in. diameter \times 0.34 in. long) for compressive creep testing.

Room temperature flexure tests were performed in 4-point bend under a loading rate of ~ 0.51 cm/min (0.2 in./min) in an Instron Universal Testing Machine. The bottom span was 3.81 cm (1.5 in.) while the top span was 1.91 cm (0.75 in.).

Elevated temperature tests were performed under an argon atmosphere in a 3-point flexure mode using a molybdenum jig. The span utilized was 3.81 cm (1.5 in.). Temperature was monitored by thermocouples located at the top and bottom of the specimen. The loading rate was again ~ 0.51 cm/min.

The breaking strength of all three materials in both the strong and weak hot-pressing directions is shown in Figure 16. It will be noted that the room and elevated temperature strength values are plotted on the same figure for convenience purposes. To compare values, Lange⁽¹¹⁾ has predicted that the mean strength measured in 3-point flexure will be $\sim 15\%$ greater than that obtained in 4-point flexural loading.

While the measured strength values are not exceptionally high, there does not appear to be a significant strength decrease as a function of temperature for

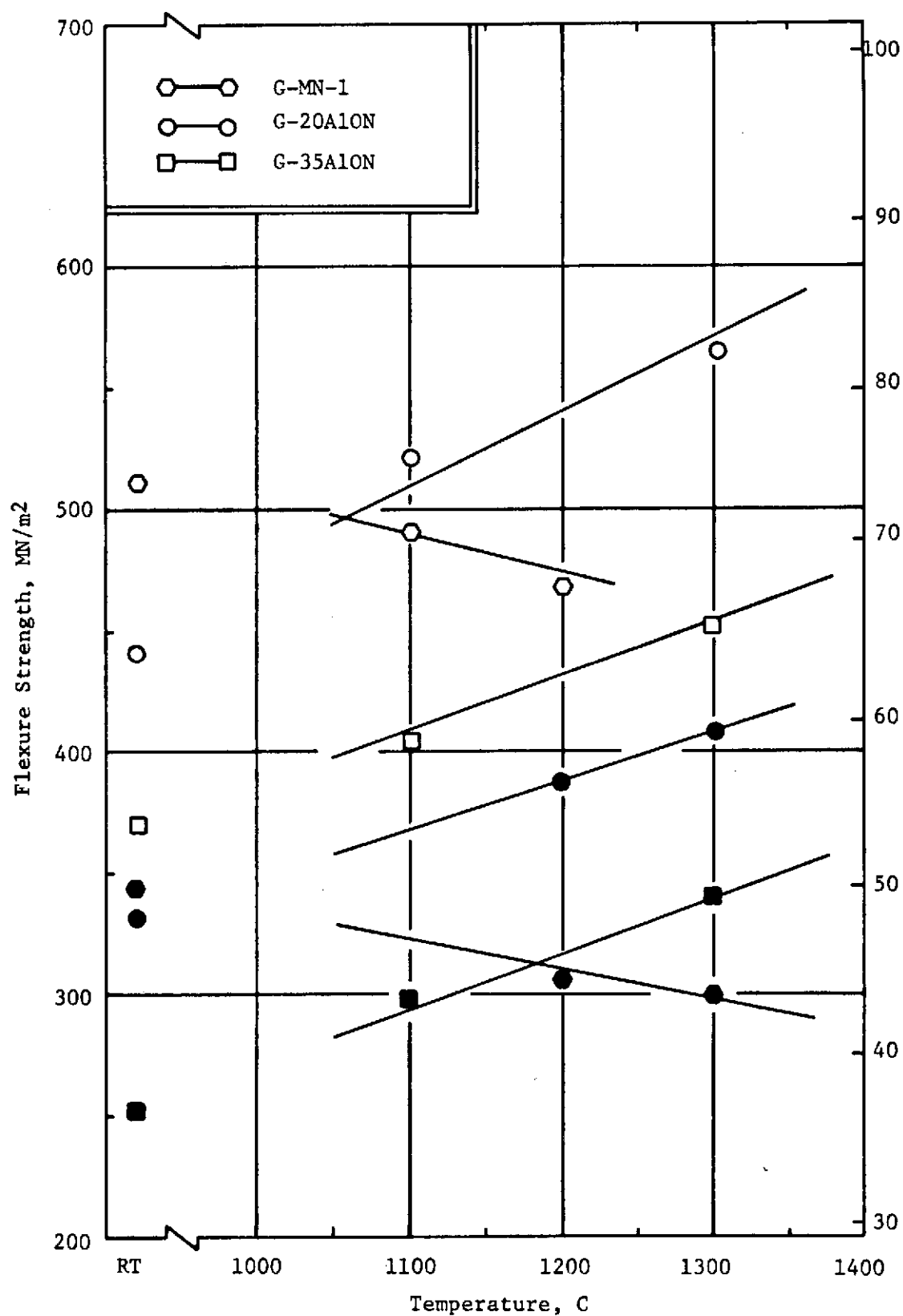


FIGURE 16. FLEXURE STRENGTH AS A FUNCTION OF TEMPERATURE
(Closed symbols represent weak hot-pressing direction, open symbols represent strong direction.)

the sialon materials. Although the strength data shown is based on an extremely small testing population, there does appear to be an upward trend in the strength as a function of temperature. Deflection was not measured. Similar observations have been made on sintered sialon materials which have also utilized a nitride additive to compensate for the grain boundary phase.⁽¹²⁾

On the other hand, the Mg_3N_2 containing specimens indicated a strength decrease as a function of temperature. It will be recalled that these specimens were porous and the strength values may not be representative of the material.

The directionality of hot-pressed silicon nitride is apparent. There is a 40-50 percent strength difference depending on the testing direction with regard to the hot-pressing direction.

While the overall strength values are somewhat low, the trends at elevated temperatures are believed to be real. It is believed that the strength values could be increased considerably by improving the powder processing (i.e. optimized milling, controlling particle size distribution, etc.). Strength values of 700 MN/m^2 ($\sim 100 \text{ ksi}$) should be achievable.

The compressive creep behavior of 20-AlON was measured in air at 1400 C. The isothermal creep as a function of applied stress is shown in Figure 17. Also shown, for comparison purposes, is the creep behavior of commercially available HS-130 Si_3N_4 tested under identical conditions. It will be noted that, under $\sim 69 \text{ MN/m}^2$ (10,000 psi), the creep rate of the HS-130 is two orders of magnitude greater than the G-20AlON material.

Preliminary measurements⁽¹³⁾ at other temperature levels indicate that a different creep mechanism is operative in the G-20AlON than in the HS-130 material. While the mechanism has not been defined, comparisons of the stress dependence and activation energy indicate that the mechanism is not grain boundary sliding as in the HS-130 Si_3N_4 . These preliminary data are believed to confirm the absence of a soft (at temperature) grain-boundary silicate phase.

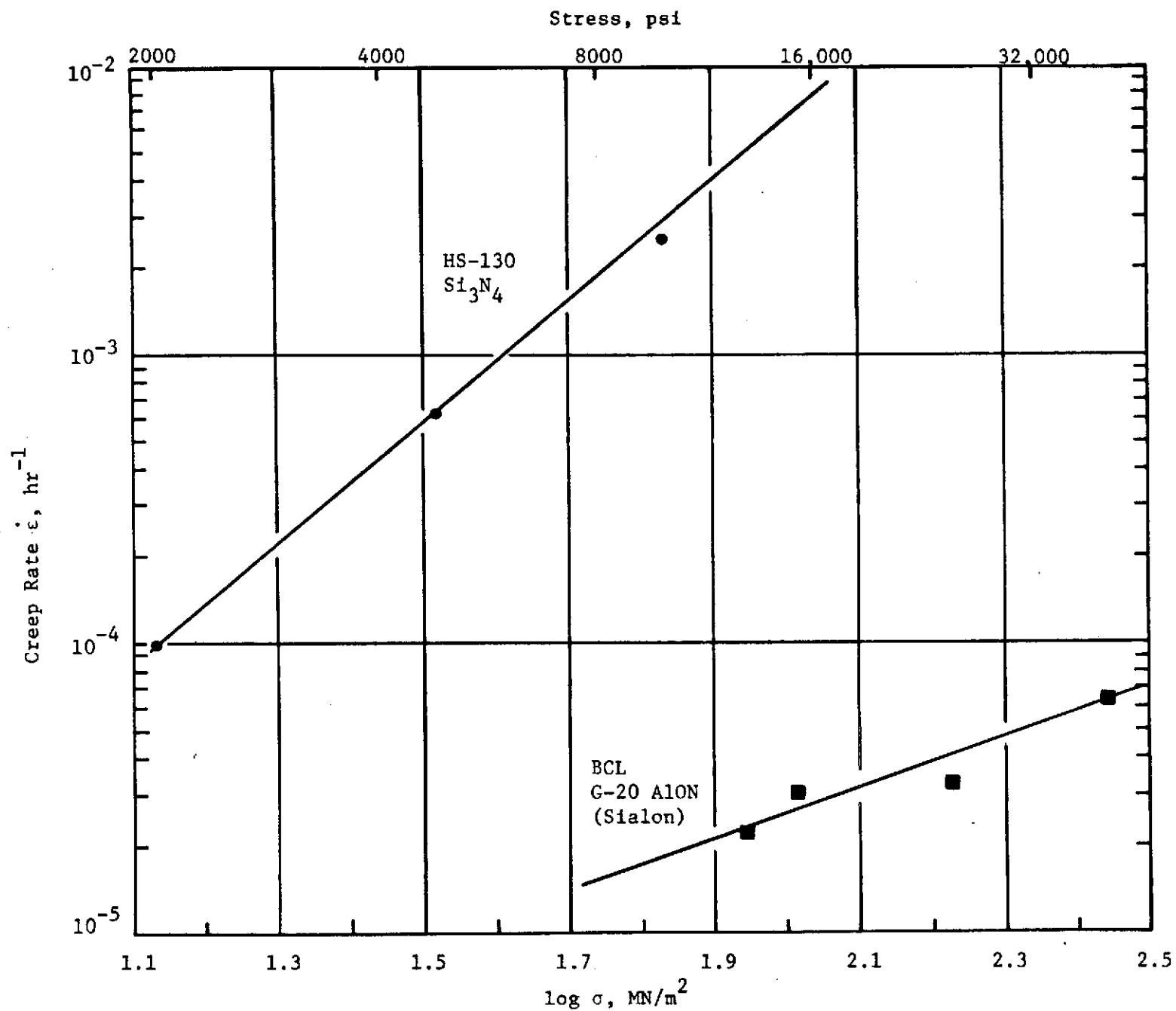


FIGURE 17. CREEP BEHAVIOR IN AIR OF BCL G-20ALON SIALON COMPARED WITH THAT OF COMMERCIAL SILICON NITRIDE (TEMPERATURE = 1400 C)

DISCUSSION OF RESULTS

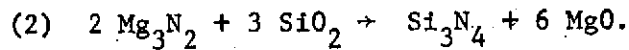
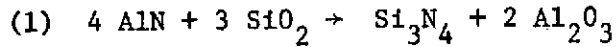
The experimental results obtained on this program appear to substantiate the concept of "grain boundary engineering". It has been demonstrated through numerous research programs that the grain boundary silicate phase is the strength limiting feature of currently available silicon nitride materials. The concept of removing a considerable portion of the natural silica by a thermal treatment coupled with the judgmental selection of additive materials to control the composition of, or completely eliminate, the silicate grain boundary phase appears to be a viable method of developing silicon nitride with improved high-temperature behavior.

The results obtained on the program indicate that it is possible to remove approximately one-half of the oxygen contamination by a 16-hour thermal treatment at 1600 C under a partial pressure of nitrogen. Once this has been accomplished, it is necessary to perform all further operations under a high-purity, inert atmosphere to prevent recontamination of the powder.

The data also indicated quite strongly that the rate of oxygen removal achieved by the above treatment was quite dependent upon the individual powder characteristics. Because powders vary considerably from supplier to supplier, individual post-treatment oxygen analysis is necessary per powder lot. It was also shown that powder quality and properties can vary considerably for the same grade from the same supplier.

In selecting additive materials which would compensate for the residual oxygen remaining in the structure following thermal treatment, nitride materials were shown to exhibit the most promise. It was shown that AlN and Mg_3N_2 were both quite effective in removal of the silica through reaction to form the nitride and the corresponding additive base-metal oxide.

It was also found necessary to incorporate the additive materials in a stoichiometric amount depending on the oxygen (silica) content of the powder according to the reactions:



When Mg_3N_2 additions are made in amounts greater than indicated from the oxygen level of the silicon nitride powder, a grain boundary phase forms which is believed to be magnesium-silicon nitride. Preliminary measurements indicate that formation of this phase will reduce the strength of the material.

Using magnesium nitride as the oxygen compensation additive produces a material which requires no further additions for achieving high density by hot pressing. This observation tends to confirm data indicating that Mg^{+2} ions lead to enhanced diffusion in the system.

The grain boundaries in the Mg_3N_2 -containing silicon nitride are believed to be comprised of MgO in solid solution with silicon nitride. As a result, grain boundary width will vary as a function of the amount of additive utilized which is a direct function of the amount of oxygen in the system. Examination of tensile strength data generated by diametrical compression tests on Mg_3N_2 -containing silicon nitrides of different oxygen levels (hence different additive levels) indicate that there is an optimum amount from a strength standpoint which could be added to the system. These data are shown in Figure 18.

The low-strength values observed at low-additive levels are due to the lack of intergranular bonding and failure to attain full density. At high-additive levels, the strength fall-off is believed due to a broadening of the grain boundaries. Figure 19 illustrates a high-oxygen silicon nitride hot pressed with Mg_3N_2 additions in stoichiometric amounts required to balance the oxygen in the system. As compared to Figure 13, prepared from low-oxygen material, the grain boundaries are much more definitive and considerably broader. Although materials containing the larger amounts of magnesium nitride are easier to densify, the strength sacrifice renders the use of high-additive levels questionable.

Aluminum nitride added alone in amounts sufficient to compensate the residual powder oxygen level does not perform as a densification aid, but does

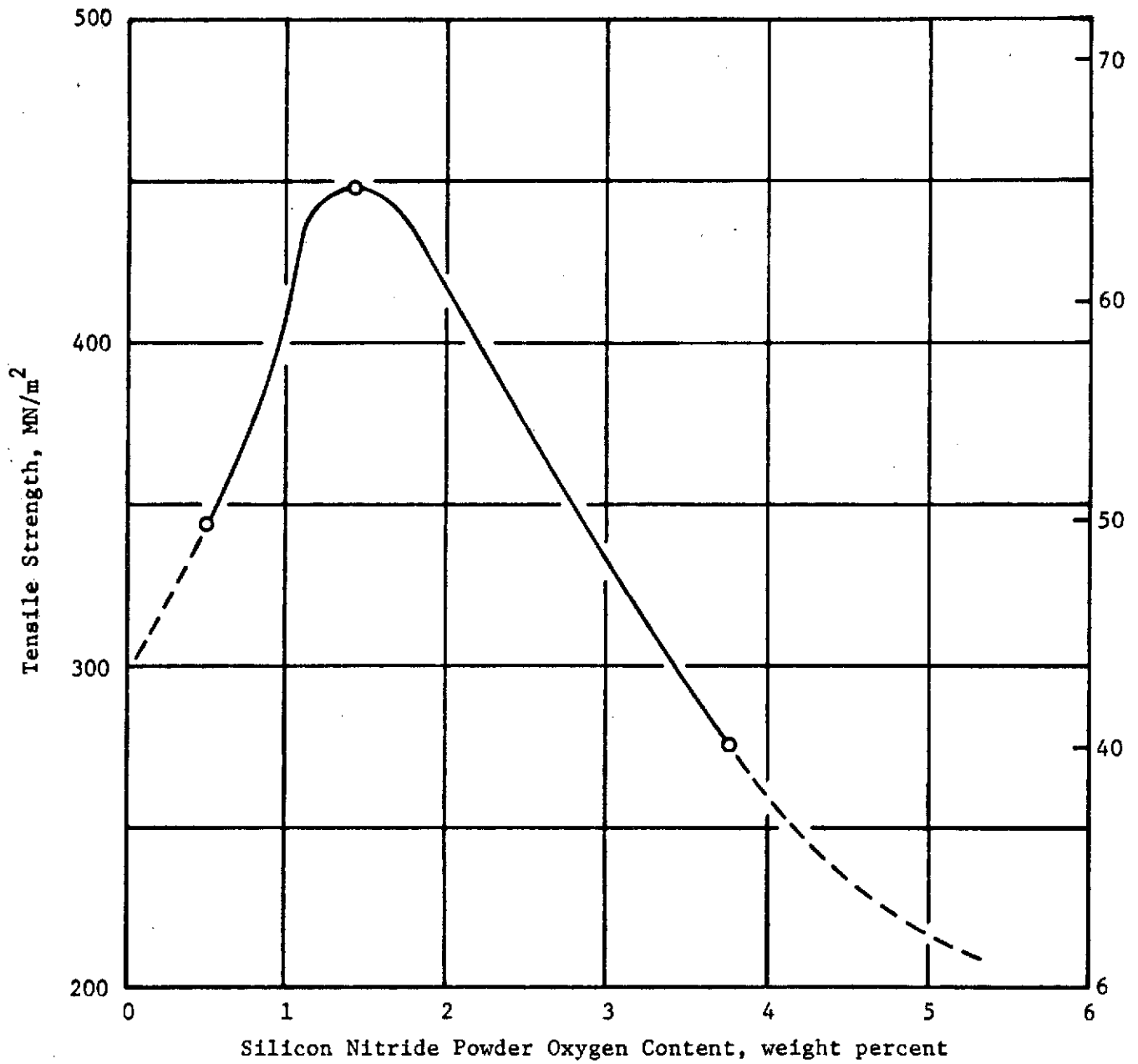
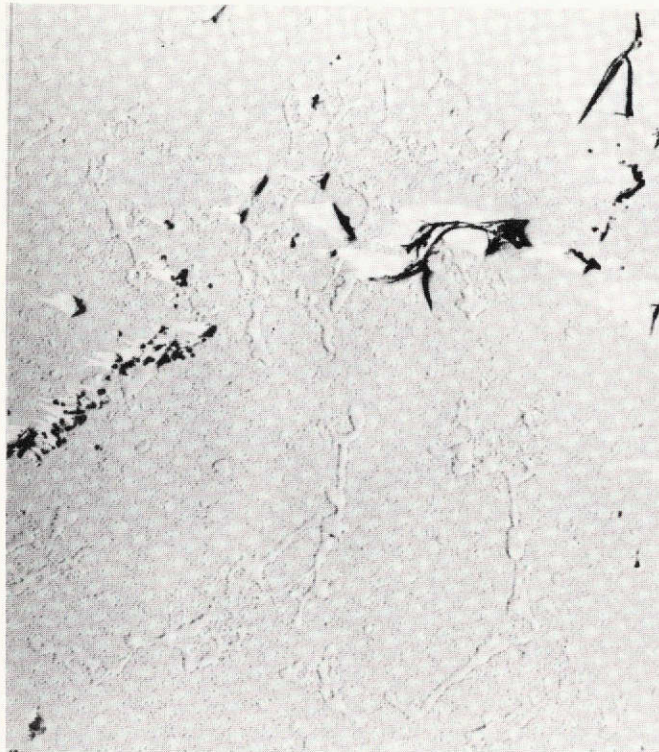


FIGURE 18. STRENGTH BEHAVIOR OF Si_3N_4 ADDITIVE AS A FUNCTION OF INITIAL POWDER OXYGEN CONTENT (Additive Level)

REPRODUCIBILITY OF THE
ORIGINAL PAGE IS POOR



12000X

EH4734

FIGURE 19. HIGH-OXYGEN SILICON NITRIDE CONTAINING
MAGNESIUM NITRIDE ADDITIVE (F2-MN-1)

Initial Powder Oxygen Level = 3.76 percent
Initial Composition = Si_3N_4 + 7.33 w/o Mg_3N_2
Density = 3.163 g/cm^3

This page is reproduced at the
back of the report by a different
reproduction method to provide
better detail.

appear to be quite effective in removing the oxide from the grain boundary. Thermodynamically, the reaction of AlN with SiO_2 to form Si_3N_4 and Al_2O_3 is very favorable; however, due to the small amount of Al_2O_3 formed, the reaction product is not sufficient to promote densification.

Aluminum nitride added in amounts greater than those required by a stoichiometric balance will not promote densification. It appears that the solid solubility of AlN in Si_3N_4 is quite limited.

Aluminum oxide added to mixtures of Si_3N_4 plus AlN performs quite well as a densification aid. The AlN is added in amounts sufficient to compensate for the residual oxygen and sufficient Al_2O_3 is then added to form a desired composition (sialon) in conjunction with the $\text{SiO}_2 - \text{Al}_2\text{O}_3$ reaction product.

Depending upon the starting oxygen content of the silicon nitride powder, the grain boundary phase appears to be of a different sialon composition than the bulk of the material. A post-consolidation thermal anneal could possibly homogenize the structure and remove the grain boundaries.

Structurally and property-wise, the oxygen compensated sialons appear quite interesting. Due to the somewhat limited scope of this program, only two compositions were evaluated. It is believed that compositions ranging from 5 to 70 mole percent Al_2O_3 in the final product should be evaluated to fully define the composition-property relationship in the system. The limited data generated on this program tended to indicate that the strength (room temperature) and elastic modulus may decrease as a function of increasing Al_2O_3 content.

From the standpoint of achieving high-impact values, the property results were somewhat disappointing. Although the structural aspects of the objectives were achieved, i.e., elimination of the strength limiting grain-boundary phase, impact values were only comparable to those reported in other investigations. In keeping with the basic premise of the investigation, this may have been due to the fact that the material did not exhibit extremely high room temperature strength.

While it is believed that the strength values could be improved to the point where the material could exhibit strength values in excess of 690 MN/m^2 (100 ksi), it is not certain that the impact would increase significantly above those values reported in this study.

Most data generated have shown that the strength of silicon nitride-base material is quite dependent upon the grinding operation and the surface finish of the structure. Specimens with a 14 rms finish were judged to be insufficient to exhibit high, 0.68 j, impact values. It is believed that target values and strength data generated on specimens with a highly idealized or optimum finish are not suitable for the generation of design mechanical property data. This type of data represents an ideal situation which is not typical of the real world to be encountered in production of components.

It appears from this study that the main advantage of the "grain boundary engineered" material lies in its high temperature mechanical behavior. Unlike the commercial grades of hot-pressed silicon nitride, the oxygen compensated sialons did not exhibit a strength decrease at elevated temperature but rather actually showed a strength increase. It is recognized that this observation was based on a limited population of specimens; however, the trend shown is believed to be real. The room temperature strength values, while not exceptionally high, could be improved and the microstructure enhanced through improved powder processing, i.e., blending, ball milling, and etc.

The limited creep data obtained demonstrated the advantage of the oxygen compensated, grain boundary engineered material. The 20 mole percent sialon exhibited a creep rate two orders of magnitude lower than HS-130 at 1400 C under 69 MN/m^2 (10,000 psi). The limited data suggest that a creep mechanism other than grain boundary sliding is operable in this material and that it indeed demonstrates a great improvement over what is currently available.

In conclusion, it is believed that the study suggests that the oxygen compensated sialons hold great promise for improving the mechanical property behavior of silicon nitride-base materials. Initial indications are that Mg_3N_2

containing materials may be too sensitive to compositions to be an effective system; however, Mg_3N_2 is quite effective in removing or compensating the grain boundary oxygen. It must be stated that the concept of grain boundary engineering does hold a great deal of promise in improving the high temperature mechanical behavior of silicon nitride-base materials.

CONCLUSIONS

Based on the results obtained and the observations on this program, the following conclusions have been made.

- (1) Approximately 50 percent of the natural-occurring oxide on the surface of silicon nitride powder can be effectively removed by thermal treatment at 1600 C under a partial pressure of nitrogen.
- (2) Aluminum nitride and magnesium nitride will effectively perform as a compensation additive for the removal of the residual silica from silicon nitride if added in stoichiometric proportions based on the amount of residual oxygen (silica) in the system.
- (3) Magnesium nitride will perform as a densification aid for hot-pressing silicon nitride as well as a compensation additive for the removal of silica.
- (4) Aluminum nitride, while performing as an effective compensation additive, will not also serve as a densification aid for hot pressing.
- (5) Silicon nitride compensated with aluminum nitride can be densified if sufficient aluminum oxide is added to the system. The minimum amount of aluminum oxide required was not defined.
- (6) Structures prepared from the magnesium nitride compensated and the dual-additive sialon materials did not meet the impact target of 0.68 j. The maximum values obtained were ~ 0.24 j at room temperature. The maximum impact values observed tended to increase slightly as a function of increasing test temperatures.
- (7) The concept of grain-boundary-engineering by complete elimination of the grain-boundary silicate phase was achieved by the thermal purification treatment coupled with the use of an oxygen compensation additive.
- (8) The advantages of grain-boundary-engineering as defined in this study are readily apparent in the elevated temperature mechanical property behavior. The dual-additive sialon materials exhibited a slight strength increase as a function of temperature as opposed to the classical strength decrease.

- (9) The creep behavior of the dual-additive sialon material is considerably better than commercially available silicon nitride at 1400 C. A grain-boundary sliding mechanism was not observed in the sialons which may be indicative of the absence of a grain-boundary silicate phase.
- (10) Of the materials investigated or developed in this study, the dual-additive sialons exhibited the most promise and are judged worthy of continued development.

RECOMMENDATIONS

In view of the promising trends indicated in the elevated temperature mechanical behavior of the dual-additive sialons, it is recommended that further studies on these materials be conducted. Emphasis should be placed on composition/ structure development to define the behavior of this material as a function of final alumina content.

It is further recommended that these studies be primarily directed toward improving the stress-rupture or creep strength of silicon nitride-base materials. Elevated temperature flexure behavior should also be evaluated along with oxidation resistance and impact behavior. It is believed that the most serious problem with present silicon nitride materials is the lack of stress rupture or creep resistance and this area should receive prime attention. The advantages of the dual-additive sialon materials for solving this problem have been demonstrated.

It is also recommended that future studies on the dual-additive sialons also include sintering as well as hot pressing as a densification technique. Sintered and hot-pressed structures should both be evaluated. Because current investigations indicate that specimens can be sintered to high density, this fabrication technique should receive increased attention.

The eventual fabrication of complex turbine components by a sintering technique is more practical, both technically and economically, than those techniques requiring the application of pressure.

REFERENCES

- (1) Wild, S., Grierson, P., Jack, K.H., and Latimer, M.J., "The Role of Magnesia in Hot-Pressed Silicon Nitride", 1970 Special Ceramics Symposium at Stoke-on-Trent, 5, Brit. Ceram. Research Assoc. (1972).
- (2) Kossowsky, R., and Frazier, W.C., Bull. Am. Ceram. Soc. (abstr), 52, 646 (1973).
- (3) Iskoe, J.L., and Lange, F.F., Bull. Am. Ceram. Soc. (abstr), 52, 646 (1973).
- (4) Terwilliger, G.R., and Lange, F.F., "Hot-Pressing Behavior of Si_3N_4 ", J. Am. Ceram. Soc., 57, [1], p. 25-29, (Jan. 1974).
- (5) Niesz, D.E., Bennett, R.B., and Snyder, M.J., "Strength Characterization of Powder Aggregates", Bull. Am. Ceram. Soc., 51, [9], p. 677-680 (Sept. 1972).
- (6) Oyama, Y., and Kamigaito, O., "Hot Pressing of $\text{Si}_3\text{N}_4\text{-Al}_2\text{O}_3$ ", Yogyo-Kyokai-Ski, 80 (8), p. 327-36 (1972).
- (7) Jack, K.H., Private Communication (April, 1974).
- (8) Oyama, Y., and Kamigaito, O., "Hot Pressing of $\text{Si}_3\text{N}_4\text{-Al}_2\text{O}_3$ ", Yogyo-Kyokai-Ski, 80 (8), p. 325 (1972).
- (9) Bennett, R.B., and Niesz, D.E., "Comminution of a Reactive Alumina Powder", Report No. 2, ONR Contract No. N00014-68-C-0342 (October. 1971).
- (10) Cannon, R.M., and Hill, R.J., "High-Temperature Compounds for Turbine Blades", NASA CR-72794, (August 31, 1970).
- (11) Lange, F. F., "Strong, High-Temperature Ceramics", Annual Review of Materials Science, Volume 4, page 370 (1974).
- (12) Wimmer, J. M., Private Communication (May, 1974).
- (13) Seltzer, M. S., Clauer, A. H., and Wilcox, B. A., "High-Temperature Creep of Ceramics", Report No. 6 ARL/LL Contract No. F 33615-73-C-4111 (August 15, 1974).

THE FOLLOWING PAGES ARE DUPLICATES OF
ILLUSTRATIONS APPEARING ELSEWHERE IN THIS
REPORT. THEY HAVE BEEN REPRODUCED HERE BY
A DIFFERENT METHOD TO PROVIDE BETTER DETAIL